January 2015

NON DESTRUCTIVE TESTING OF SOFT BODY ARMOR

Karan Bhise
Purdue University

Graduate School Form 30
Updated 1/15/2015

PURDUE UNIVERSITY
GRADUATE SCHOOL
Thesis/Dissertation Acceptance

This is to certify that the thesis/dissertation prepared

By KARAN NITIN BHISE

Entitled

NON DESTRUCTIVE TESTING OF SOFT BODY ARMOR

For the degree of Master of Science in Aeronautics and Astronautics

Is approved by the final examining committee:

WEINONG WAYNE CHEN
Chair

CHARLES ROBERT KENLEY

VIKAS TOMAR

To the best of my knowledge and as understood by the student in the Thesis/Dissertation Agreement, Publication Delay, and Certification Disclaimer (Graduate School Form 32), this thesis/dissertation adheres to the provisions of Purdue University's "Policy of Integrity in Research" and the use of copyright material.

Approved by Major Professor(s): WEINONG WAYNE CHEN

Approved by: WEINONG WAYNE CHEN 11/23/2015

Head of the Departmental Graduate Program Date

NON DESTRUCTIVE TESTING OF SOFT BODY ARMOR

A Thesis

Submitted to the Faculty

of

Purdue University

by

Karan Bhise

In Partial Fulfillment of the

Requirements for the Degree

of

Master of Science in Aeronautics and Astronautics

December 2015

Purdue University

West Lafayette, Indiana

ACKNOWLEDGMENTS

First and foremost, I would like to convey my gratitude to my advisor, Professor Weinong Chen, for his support throughout my thesis at School of Aeronautics and Astronautics, Purdue University. With his status as one of the leading researchers in the field of Structures and Impact Science, it has been a privilege to perform research under his supervision in the short period of time that we worked together. He has always been supportive, helpful, filled with ideas and a very understanding advisor making my research experience a memorable one.

I would sincerely like to thank Dr. Philipp Seiler for being a mentor, a guide, a friend and a great helping hand throughout the term of my research. Without him, I would not have completed my tasks successfully in the stipulated amount of time. He not only helped me get out of deadlocks in my research but also provided me with helpful tips to improve my efficiency. His insights aided me in looking at different aspects of the problem, thus helping me to answer all the questions related to specific problems.

Next I would like to extend my appreciation for Niranjan Parab, Matthew Hudspeth and Ben Claus for developing the main idea of the project without which this project would not have existed. Most importantly I would like to thank Jongseong Choi and Boon Him Lim for working with me in tandem to achieve the required objectives and complete the given tasks on time with utmost satisfaction.

I sincerely thank Dr. Vikas Tomar and Dr. Charles Kenley for making time from their busy schedule and helping me towards the completion of my thesis. I would also like to extend my gratitude to Linda Flack, Jennifer Laguire and all others from School of Aeronautics and Astronautics who made sure my stay at Purdue was hassle-free. Finally a big thanks to my parents, family and all friends within and outside

Purdue who helped and motivated me during my stay at Purdue and successfully accomplish my goals as a graduate students.

TABLE OF CONTENTS

LIST OF TABLES

LIST OF FIGURES

SYMBOLS

g	Grams
mm	Millimeters
m	Meters
ft	Feet
s	Seconds
lbs	Pounds
lbf	Pound Force
in	Inches
V	Final Velocity
U	Initial Velocity
g	Acceleration due to Gravity
H	Height
psi	Per Square Inch
cm	Centimeter
kg	Kilogram
GPa	Giga Pascals

ABBREVIATIONS

IACP	The International Association of Chiefs of Police
VEST	Vibration Energy Signature Test
RAND	Research and Development
ACP	Automatic Colt Pistol
LR LRN	Long Rifle Lead Round Nose
FMJ RN	Full Metal Jacketed Round Nose
SIG	Susquehanna International Group
FFT	Fast Fourier Transforms
DFT	Discrete Fourier Transforms

ABSTRACT

Karan, Bhise MSAA, Purdue University, December 2015. Non Destructive Testing of Soft Body Armor. Major Professor: Dr. Weinong Chen.

Pristine bullet proof vests are extremely effective at halting pre-determined projectile threats and have saved over 3000 lives [1]. However, the effectiveness of these vests to halt a bullet is seen to decrease over time. Owing to the importance of bullet proof vests over a period of time, tests to determine their effectiveness have been carried out on every batch of vests at the time of inception and at certain time intervals by shooting a bullet through them. A few vests from every batch are picked up and shot at to check for bullet penetration during this process while these results are extrapolated onto the other vests from the batch.

One of the main issues with this method is the fact that testing a few jackets among a large set of jackets does not guarantee the safety of every jacket in the entire batch. Further the jackets that are shot-at have the possibility of undergoing substantial damage during the process thus compromising its safety rendering them unsafe for future use. As the vest penetration phenomenon is extremely complex too, there arose a need for a better testing procedure that could not only help ensure more safety, but also save time and money.

The new testing procedure proposed a non-destructive evaluation of the jackets that would solve the issues previous faced in testing the vests. This would lead to the building of a portable set up which could be carried to any location to test jackets in a matter of minutes thus saving time and money.

1. Introduction

1.1 Definition of Body Armor

The term - Body Armor is generally related to vests worn for ballistic and stabbing protection to important body parts like the heart, liver, kidney and so on in the torso. Usually, a vest contains two armor panels held in place by a a cover material. One of the panels protects the front of the torso, the other protects the rear. In order to protect the sides of the torso, the vest is worn with the front panel overlapping the rear panel. Any of these panels can be removed from the carrier based on the need. [2] Soft vests are made from many layers of woven or laminated fibers in modern days and are capable of protecting the wearer from small-caliber handgun and shotgun projectiles, and small fragments from explosives such as hand grenades.

Armor has been in use for a very long time since the stone age beginning with hides, leather, bone, moving on to metals like bronze and steel, later coming to ballistic cloth, ceramics, and recently, depleted uranium. Among the latest armor development, also called as the bullet proof vest, has primarily been a way to protect oneself from harm in combat and military engagements. Currently, the typical military personal armor system includes a kevlar vest manufactured by DuPont company, with or without ceramic inserts, and a military helmet. [3]

Metal or ceramic plates have been traditionally used with a soft vest to provide an additional protection from rifle rounds, while metallic components or tightly knitted woven fiber layers have provided soft armour resistance to stabbing and slash attacks from knives and other similar weapons. Soft vests are commonly worn by police forces, other personnel who are at risk of being shot like political and national leaders, security guards, and bodyguards, whereas hard-plate reinforced vests are mainly worn

by combat soldiers, police tactical units, and hostage rescue teams who encounter projectiles of higher velocities.

Bullet proof vests use layers of strong fibers to hold and deform a bullet, remoulding it into a dish sort of shape, and spreading its force over a larger portion of the vest fibers. The vest, in this process, absorbs most of the energy from the deforming bullet, bringing it to a stop before it can fully penetrate the textile matrix structure. Some layers may be penetrated but as the bullet goes on deforming, the energy is dissipated and keeps getting spread over a larger and larger area.

While a ballistic vest can prevent bullet penetration, the vest and wearer still absorbs the bullet's energy. Even with no penetration as such, modern bullets shot from pistols possess enough energy to cause blunt force trauma right around the impact location. Vest specification typically include both penetration resistance requirements as well as limits on the amount of impact energy that is delivered to the body. Vests designed for bullets offer little protection against blows from sharp implements generally, such as knives or arrows, or from bullets manufactured of non-deformable materials, e.g., those containing a steel core instead of lead. This is because the impact force of these objects stays concentrated in a relatively small area as these objects are not deformed on impact, allowing them to puncture the fiber layers of most bullet-resistant fabrics.

Textiles are added with metal (steel or titanium), ceramic or polyethylene plates at times with an intention to provide extra protection to important areas. These hard armor plates have been effective against mostly all the handgun bullets and a variety of rifles. These manually upgraded ballistic vests are typically standard in military use because of the fact that the soft body armor vests are ineffective against military rifle rounds. Prison guards and police often wear vests that are designed for protection against bladed weapons and sharp objects which are also considered to be the primary source of attack for such personnel.

Figure 1.2 on shows some ancient body armor that was used before an extensive study of armor materials started in the twentieth century. The main difference be-

tween ancient armor and today's armor is the material used which has a direct impact on the weight of the armor. In ancient times the armor was built from metals which made it heavier and thus the wearer was not as mobile as personnel wearing lighter vests today. Further ancient vests at times covered the whole body which is different from vests manufactured these days.

1.2 Importance of Body Armor

A look into statistics to see the importance of body armor, it has shown to have saved a number of lives over time. However it is statistically expected that this number saved each year would be way more than the present account if every personnel wore armor at all times during duty. Wearing armor not only saved wearers from death by firearms but also protects them from fatal injuries in other types of assaults and accidents. [4]

Body armor is one of the most important pieces of safety equipment used by officers. Owing to the FBI Uniform Crime reports of 2011, it was noted that as many as 1,800 and 2,300 officers were attacked with firearms every year from 2002 to 2011. [5] Among the 543 officers killed during this particular period, about 498 of them were killed with firearms [6]. In 2011 alone, 72 officers were feloniously killed out of which as many as 63 were killed with firearms. Modern police body armor was introduced into practice in the 1970s as a result of NIJ-funded research. The International Association of Chiefs of Police (IACP)/DuPont Kevlar Survivors Club have successfully recorded more than 3000 instances of officers being saved since then because they wore body armor. RAND had published a report in the year 2010 which presented a very interesting statistic. It indicated that an officer without the body armor, on an average, was three and half times more susceptible to a fatal injury if shot than the counterpart wearing body armor. [7] Figure 1.1 shows the number of deaths of officers by firearms (officers without body armor) and other means in order to depict the importance the body armor has in saving the lives of police officers.

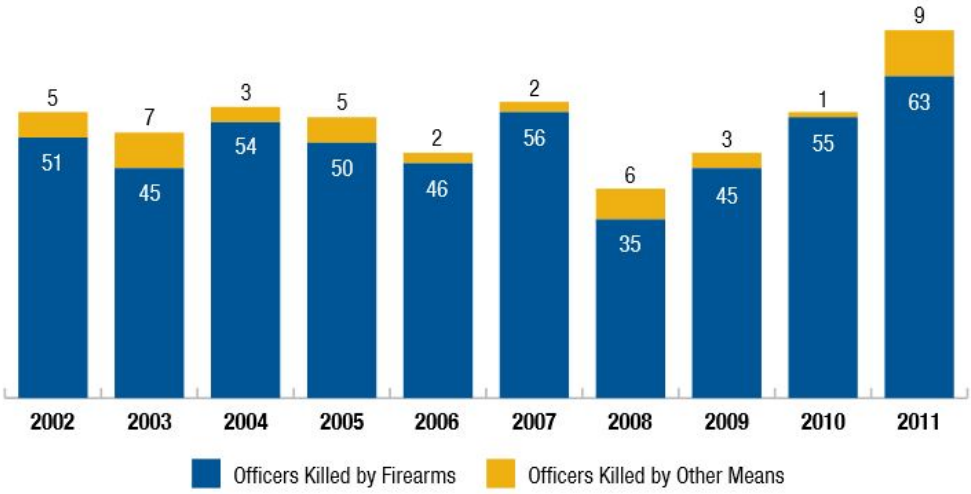

Figure 1.1.: Officers Feloniously Killed between 2002 and 2011 [6]

1.3 History of Body Armor

Protecting oneself from threats is a human instinct and people have always been trying to save themselves from any kind of injury with the help of external sources. Among the primitive materials used, a few of them used animal skins or their hides to protect themselves from attacks. As weaponry became more and more modernized and developed, they added reinforcements in the form of metal shields or wooden plates to their defensive mechanisms.

During the 'Stone Age', humans used thick animal hides for dual purpose including clothing and protection. This was the first development of body armor in the history of mankind. As time passed, they developed the need and use of wooden plates or metals to protect ones body. A system of segments were assembled with metal straps and used for protection by the Roman soldiers. This system was named as Lorica which is Latin for armor. Around the fifteenth and sixteenth century, with the advancement and excessive use of firearms for attacks, that type of protective clothing was no longer a safe option. In the late 19th century, the military wanted to look into soft armor as an improvement of the current armor. This as surely a

very effective option against low-velocity bullets,however failed to protect the wearers against the new generation of weapons. [8]

(a) German Plate metal from the 16th century.

(b) A medieval knight with his horse, his armor, and his weaponry.

Figure 1.2.: Ancient Body Armor [9]

It was the Japanese that first decided to look into soft and light armor as a source of improvement over the current armor. They first developed the armor from silk. This garment was made of no other material than about 30 layers of silk. These silk garments proved to be quite effective but also expensive. After President William McKinley was assassinated in 1901, the US military started to look into the soft armor as well considering it a means of precaution with mobility. These garments made of silk were shown to be effective against low-velocity bullets, however it proved to fall short in front of new generation of handgun ammunition which was expected due to lack of stiffness. The US military decided to not carry on with silk armor because of this particular reason and due to the fact that silk was very expensive.

The "flak jacket" was first invented during World War II. It was primarily made from ballistic nylon and provided protection from ammunition fragments. Flak jackets were seen to be quite bulky and ineffective against most rifle and pistol fire, but they were widely used, as they made the soldiers to feel secure by providing some modicum of protection.

In the 1960s the National Institute of Law Enforcement and Criminal Justice decided to revisit the concept of light weight body armor that police officers could wear on duty and started its research for the same. This research was able to identify a number of new materials that could be woven together, which were light weight and had ballistic resistant that was excellent if not better than metals used. After conducting the research, the agency believed that it was possible to make body armor from light materials that could be worn by police officers on patrol always. [8]

The National Institute of Law Enforcement and Criminal Justice worked in conjunction with the Bureau of Standards and came up with some type of benchmark or reference for the performance that would define ballistic resistant requirements for the body armor that could be worn by the personnel involved. The greatest achievement of the 70's among all the studied, researched and tested products was the development of the armor used by the police made from Kevlar by the DuPont company. Kevlar was originally produced with its main intention to replace the steel belting in tires. Between 1971 and 1976 the National Institute of Justice put a huge amount of money as high as 3 million dollars into the development of body armor.

This process was a four phase program that spanned several years. [8]

Phase I - Testing of Kevlar to determine its effectiveness of the material to stop the bullets from hurting the officers or not. [8]

Phase II - Here the program established how many Kevlar layers it would take to prevent the penetration of bullets of varying calibers, velocities and proposed the need to design a sample vest that would protect officers from the common bullet threats like .38 specials and .22 long rifle ammunition. By 1973 a finally a vest was developed that had seven layers of Kevlar overall that was designed for testing. [8]

Phase III - This mainly involved the medical testing and finding body armor types that would be needed to save officers lives based on the types of firearms and ammunitions used.

It was evident from the study that even if Kevlar stopeed the bullet easily, the shockwave which the bullet caused would leave an injury from a serious bruise to something as serious and fatal as damage to the critical organs in the torso. [8]

Phase IV - This section of the program made the evaluation of the body armor wearing ability and its effectiveness. This test was conducted in a few towns for the verification of the vest being wearable without hampering any kind of normal body movement that would interfere with normal police activities. In 1975 a profound research with 15 police departments serving a number of civilians as big as 250,000 and having officer assault rates much higher than the national average was carried out. Some evaluated parameters during this intense study included the comfort of the personnel while wearing a vest through an entire shift, and the adaptation of the officers to the vest in extreme temperatures. The study also involved a research on vest durability. [8]

In 1976, researchers finally concluded that Kevlar was effective in being bullet-resistant, wearable and light enough for police officers to wear full-time. Since that time bulletproof vests have improved. Currently, a level IIIA bulletproof vest on an average weighs approximately five and half pounds and can protect the wearer from almost all handgun rounds if not other advanced weapons. According to the International Association of Chiefs of Police, bulletproof vests have saved over 3,000 officers' lives since 1987. [10]

1.4 Types Of Body Armor

Many different types of armor are available ranging in ballistic resistance from those designed to protect against small caliber handguns to those designed to protect against high-powered rifles. The ballistic threat posed by a bullet depends on its

composition, shape, caliber, mass, and impact velocity among other things. Because of the wide variety of cartridges available in a given caliber, and due to the existence of hand loads, armors that would generally beat a standard test round may not defeat other loadings in the same caliber. For example, an armor that would prevent penetration by a 357 Magnum test round may or may not defeat a 357 Magnum round with higher velocity. In general, an armor that defeats a given lead bullet may not resist penetration by an identical round with a harder core. [2] So it seems necessary to classify body armor based on use.

1.4.1 Classification

Police body armors covered by this standard are classified into six types, by level of performance. These different types are described below [11]:

- **Type I (.22 LR; .380 ACP)**: This type of armor provides protection against the .22 long rifle lead round nose (LR LRN) bullets with a nominal mass of 2.6 g having a minimum impact velocity of 320 m/s (1050 ft/s) or less, as well as against the .380 ACP full metal jacketed round nose (FMJ RN) with a nominal mass of 6.2 g having a minimum impact velocity of 312 m/s (1025 ft/s) or less. Type I body armor is pretty light.

- **Type IIA (9 mm; .40 S-W)**: This armor mainly protects against the 9 mm full metal jacketed round nose (FMJ RN) bullets with a nominal mass of 8.0 g and a minimum impact velocity of 332 m/s (1090 ft/s) or less, and .40 S-W caliber full metal jacketed (FMJ) bullets having a nominal masses of 11.7 g, with a minimum impact velocity of 312 m/s (1025 ft/s) or less. It also provides protection against Type I threats as they are generally at a lower velocity.

- **Type II (9 mm; .357 Magnum)**: This armor protects against the 9 mm full metal jacketed round nose (FMJ RN) bullets with a nominal mass of 8.0 g, impacting at a minimum velocity of 358 m/s (1175 ft/s) or less, and .357 Magnum

jacketed soft point (JSP) bullets, with a nominal mass of 10.2 g, impacting at a minimum velocity of 427 m/s (1400 ft/s) or less. It also provides protection against Type I and Type IIA threats.

- **Type IIIA (.357 SIG; .44 Magnum)**:This armor provides protection against 9 mm full metal jacketed round nose (FJM RN) bullets with a nominal mass of 8.0 g, impacting at a minimum velocity of 427 m/s (1400 ft/s) or less, and .44 Magnum jacketed hollow point (JHP) bullets, with nominal masses of 15.6 g, impacting at a minimum velocity of 427 m/s (1400 ft/s) or less. It also provides protection against most handgun threats, as well as the Type I, II-A, and II threats.

- **Type III (Rifles)**: This armor provides protection against 7.62 mm full metal jacketed (FMJ) bullets with a nominal mass of 9.6 g, impacting at a minimum velocity of 838 m/s (2750 ft/s) or less. It also provides protection against Type I through III-A threats.

- **Type IV (Armor Piercing Rifle)**: This armor protects against .30 caliber armor piercing (AP) bullets with a nominal mass of 10.8 g, impacting at a minimum velocity of 869 m/s (2850 ft/s) or less. It also provides protection against the Type I through III threats. Type IV body armor provides the highest level of protection currently available. It often uses ceramic materials. As with Type III armor, Type IV armor is clearly intended only for tactical situations when the threat warrants such protection.

In this project we planned to look at projectiles from Type I to Type III only.

1.5 Motivation for the Project

1.5.1 Current Testing Procedure

Since the development of soft body armor after World War II, numerous lives have been saved in both the military and constabulary realms. Thus, understanding of a specific vest's reliability during its span of use was vital to user security. As vest efficacy was only determined before manufacture [12], in-situ analysis of vest reliability was non-existent.

However, we know that once the vest has been in use, it could be subjected to wear and tear due to both Mechanical factors like being subjected to folding, stretching and rubbing as well as environmental factors like being subjected to humidity, sweat and ultraviolet light. These factors were major causes for the deterioration of the efficiency of the body armor and a vest that was once safe against some firearms was not necessarily so safe down the line in a few years. This led to the idea of developing a technique to monitor the performance of the vests on a timely basis without affecting its safety and efficiency thus leading to the development of the idea of this project. **??**

The current testing procedure involved the destructive testing of the body armor by strapping it to a support and shooting bullets through the jacket as shown in the figure 1.3. Based on the configuration of the vests, these jackets underwent appropriate strapping after which bullets were shot at them in order to verify their effectiveness.

The main issues with this method were as follows:

- Testing few jackets from a large batch did not guarantee the safety of every jacket in the set.
- The jackets that were shot-at might underwent some damage during the process thus reducing their safety. This rendered the tested jacket unsafe for use.

As the vest penetration phenomenon was extremely complex too, a better testing procedure would not only help ensure more safety but also save time and money. This

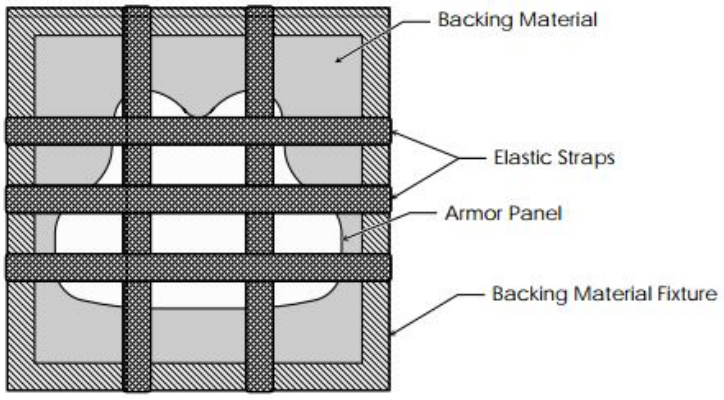

(a) Standard Strapping Arrangement for Smaller Samples

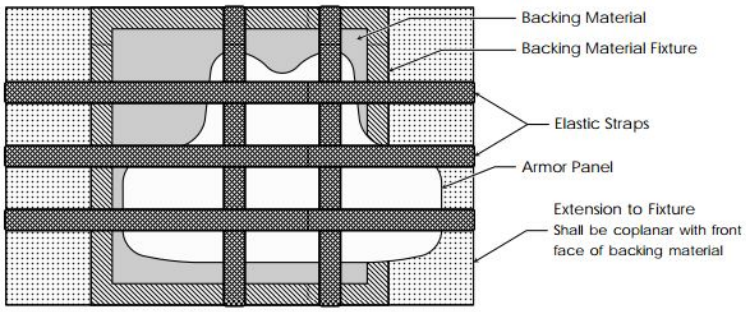

(b) Standard Strapping Arrangement for Larger Samples

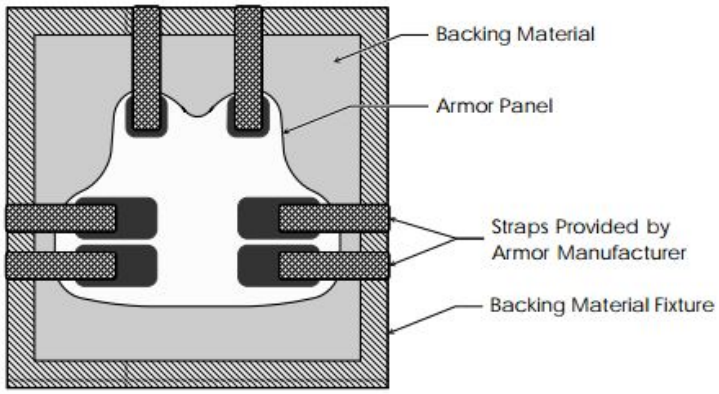

(c) Special Strapping Arrangement Using the Armors Strap Attachments

Figure 1.3.: Acceptable Strapping Methods for Body Armor [12]

(a) Bullets shot at body armor

(b) Previously Shot Armor

Figure 1.4.: Bullets shot at body armor

new testing procedure proposed a non-destructive evaluation of the jackets taking care of the issues previously faced in conventional testing.

Figure 1.4 showed a random example of a bullet proof vest strapped and shot at with the bullet impressions on the backing materials. This was an example of the trauma an officer's body underwent even when the bullet did not penetrate through the body armor. The spots designed to undergo bullet impact were shown in figure 1.5. This figure showed the positions that were strategically selected to be shot at on a vest to carry out its analyses. These locations remained constant as every such test carried out involved the same shooting locations in order to maintain the repeatability of results.

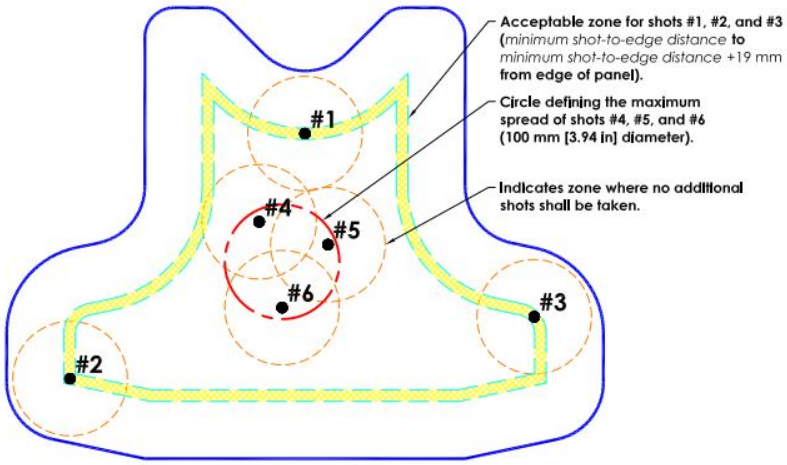

Figure 1.5.: General armor panel impact locations (front and back)

1.5.2 Non Destructive Testing Procedure

Ideally, a non-destructive evaluation test that was planned to be set in this project, would be performed throughout the life of the vest, thereby allowing for a more appropriate determination of vest longevity, rather than solely relying on the manufacturer's guarantee. This would thereby allow for a more effective means of determining a vest's threat halting efficacy throughout its life, and ultimately a safer and more productive law-enforcement personnel. This Non-Destructive Testing method would be able to adequately determine the relative stiffness governing armor efficacy and would have allowed for vests to be quickly and effectively analyzed so as to either re-instate their usage to the appropriate personnel or deem them unfit for further use in the ballistic application in which they have been designed.

1.5.3 Fast Fourier Transforms

Fast Fourier transforms are widely used for many applications in engineering, science, and mathematics. The basic ideas were mainly popularized around 1965, but some algorithms have been said to be derived as early as 1805. [13] In 1994 Gilbert

Strang went to an extent to describe the FFTs as the most important numerical algorithm of our lifetime [14] and it was also among the top 10 algorithms of 20th Century by the IEEE journal Computing in Science and Engineering. [15]

A "Fast Fourier transform (FFT) algorithm computes the Discrete Fourier Transform (DFT) of a sequence, or its inverse." Fourier analysis converts a signal from its original domain (often time or space) to a representation in the frequency domain and vice versa. An FFT rapidly computes such transformations by factorizing the DFT matrix into a product of sparse (mostly zero) factors. [16]

Here, in this project, we planned to convert the Force over Time histories to their corresponding Fast Fourier Transforms as a source of prediction of the safety of the vests. Even though a detailed study of the exact physics behind these FFTs is needed to understand them better which forms the topic of future work, the amplitudes and their corresponding frequencies provided a fair explanation of the behavior of the materials studied. These Fast Fourier Transforms plots in the Results and Discussion chapter provided more information about these analyses. Figure 1.6 shows an example of converting a Sine Wave signal to its Power Spectrum using it's Fast Fourier Transforms. The matlab script for the following conversion is shown in appendix A.

In addition to the basic Fast Fourier Transforms, a *detrend* function was used in order to plot the Fast Fourier Transforms. The *detrend* function did nothing but remove the best straight-line fit linear trend from the data in the set of values and returned back the values. This was nothing but removing the mean value curve from the force data from the analyses and returning the remaining curve to build the FFTs. This function was used because on the strange behavior seen when the FFTs were plotted where maximum amplitude values were spotted at 0 Hz frequency. In order to counter that the *detrend* function was used.

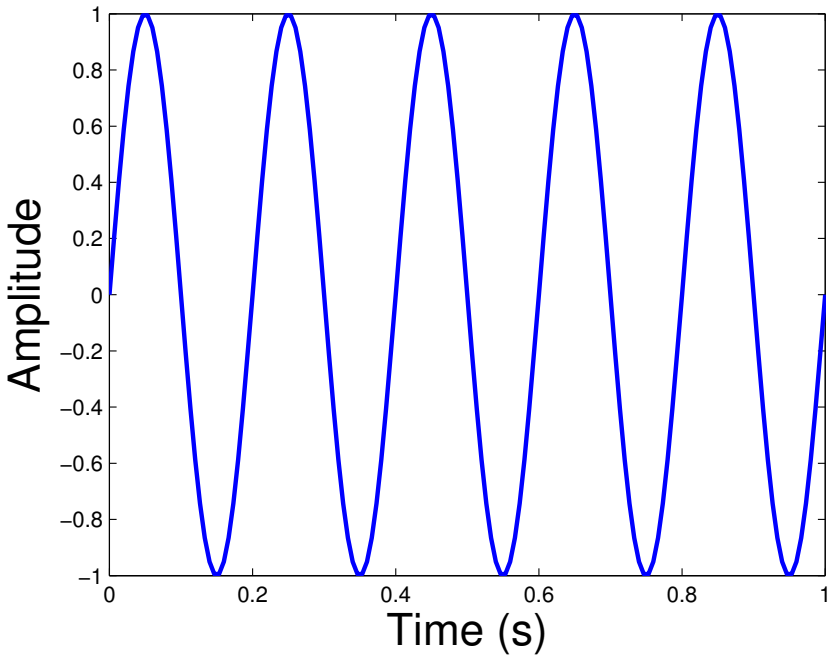

(a) Sine Wave Signal

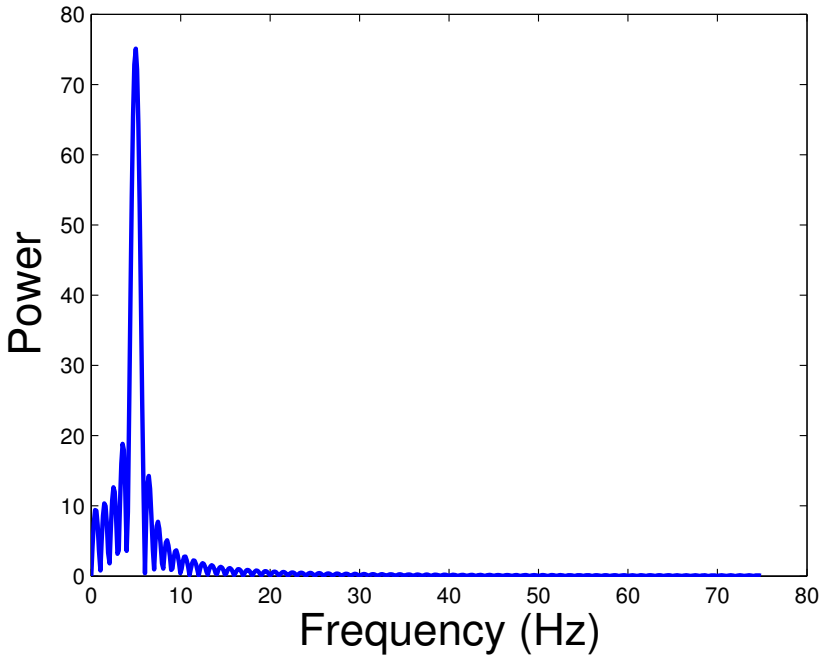

(b) Power Spectrum of a Sine Wave

Figure 1.6.: Example Showing the Use of Fast Fourier Transforms

2. Method

The methods section gives an overview of the entire process used to carry out the experimental procedure as well as its corresponding Finite Element validation.

2.1 Project Objectives

After establishing the importance of timely testing of body armor, the next step was the need to develop a Non-Destructive testing method for the same. The main objective of the project was to build a portable apparatus that could test each and every body armor at any police department or any location in a matter of minutes with a simple assembly. The final output of this apparatus was expected to be a red/green light display giving the ultimate Go-No-Go on the tested armor.

In order to achieve that, the main intention was to create a link between the hammer impact or a drop tower impact (low velocity impact) on a vest and the corresponding bullet impact (high velocity impact) and find a correlation in the behavior of these two different phenomena. The initial guesses for striking this correlation were assumed to be the study of force over time histories and their corresponding Fast Fourier Transforms. Once this correlation was obtained, the next step was to study vests over a period of time and study their responses in the newly arranged set-up. Once a parameter for safety was established through a detailed study of a new vest and the same vest after ageing, this apparatus would be used to determine the safety and effectiveness of the armor. The software in the apparatus was supposed to take care of the red/green light flashing based on the response of the tested armor to differentiate a safe vest from an unsafe one.

In order to set-up an experiment, it was necessary to validate the experimental set-up before building the portable apparatus. This would not only provide accuaracy

in the experimental set-up but also save time and money rather than building a prototype and testing for issues. In order to achieve this, it was decided to build a Finite Element Model for the proposed experimental set-up as a means to validate it.

2.2 Primary Objectives

This project was named Vibration Energy Signature Test (VEST). During the first year of this project the main aim was to validate the hammer impact tests and suggest the necessary changes to make the set-up more robust and reliable. It was necessary to create a bridge between the two methods, namely the bullet impact and the hammer impact by some kind of an interlinking principle. However, the primary objective during the first phase of the project was to provide a validation to the hammer impact experiment through an accurate Finite Element Model and also predict small variations that could help in providing a better, simpler set-up while keeping the physics and concepts of the experiment unchanged.

After studying the initial experimental set-up, the main task was to replicate the entire process on a software package that could simulate the entire experiment replicating it physically and conceptually. The following objectives were looked at during the term of this project:

- Comparison of force over time histories for a set of different materials.
- Assisting in the experimental set-up by providing a sensitivity analysis of load cell results by varying the impact point in the set-up under study.
- Effect of weight of the frame on the experimental results.
- Providing the necessary changes in the arrangement needed for an improvement

In an attempt to validate the experimental set-up, it was decided to replace the actual vest with a steel or aluminium plate. This was mainly because these plates were homogeneous isotropic materials making validation easier to study as compared to complex vest materials involving composite materials/ceramics/metal plates.

2.3 Experimental Approach

The Vibration Energy Signature Test (VEST) was planned to be performed at the state/local law enforcement level, being defined as a simple and cost/time efficient test which could determine a soft armor's insert relative stiffness. In order to ensure the correctness of the proposed technique, a prior vest evaluation was planned to study the new and old vests in order to ascertain cut-off parameters to be involved in determining the difference in behavior of the vests under study. Methods to ascertain these parameters were to be determined first by an external testing program, which would then transition the acquired method proposed to be set-up. [1]

2.3.1 Vibration Energy Signature Test (VEST)- Conceptual

The following test apparatus was proposed in the proposal in order to proceed towards building the proposed Non Destructive testing apparatus which was assumed to be a time and money saving set-up. The proposed general VEST procedure and apparatus could be seen in the figure 2.1.

The VEST apparatus consisted of fast response quartz load cells on which the vest package and the frames holding the package rested. The two frames were clamped together with the help of bolts sandwiching the vest in between. This approach was sought to provide for negligible error in clamping pressure, which could have altered the effectiveness of fabric in a ballistic environment [17]. In order to ensure negligible material pretension effects [18] throughout various tests, the bullet-proof vest was solely laid down onto the base fixture and flattened by a top and bottom circular steel flatteners to ensure no fabric wrinkling.

The set-up was then impacted in the middle of the fabric with the instrumented test hammer or a drop tower with a gravitational force on a drop tower (hammer replacement) with a self weight of 15.4 lbs. This hammer was dropped from a height of 2 in so that the velocity at the impact point is 1 m/s. This was calculated from the Second Equation of Motion (Accelerated Motion) given by:

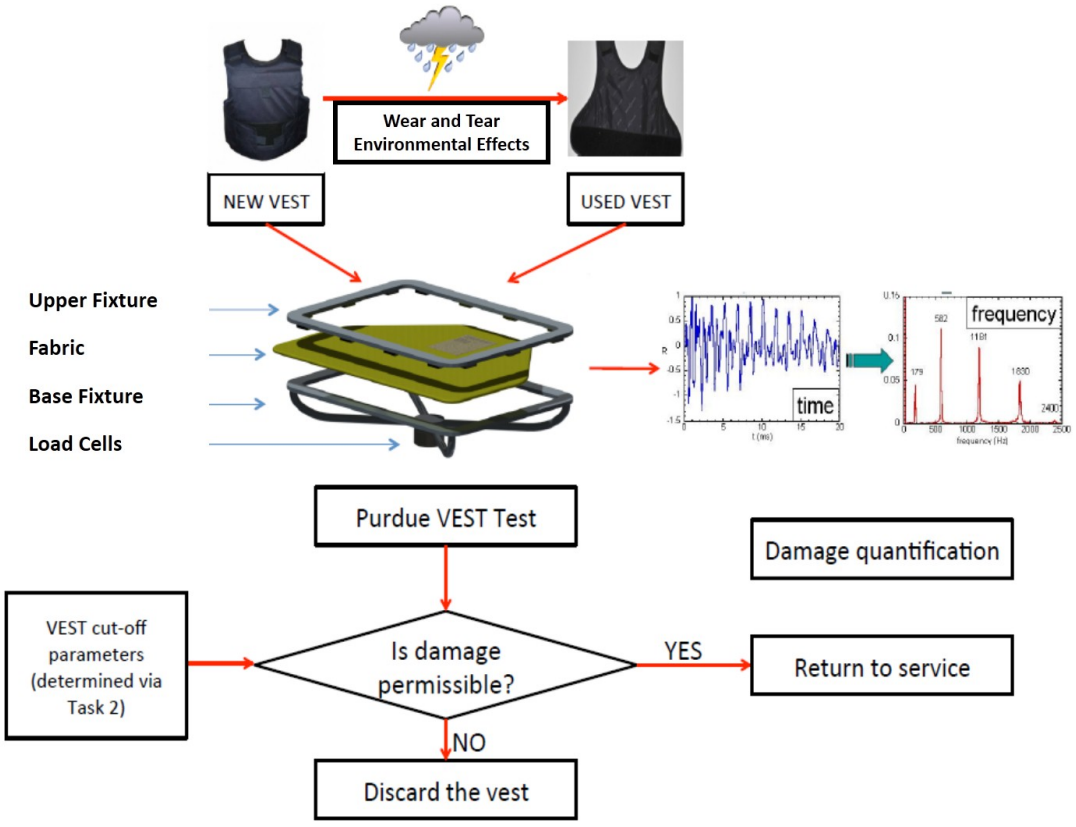

Figure 2.1.: VEST Experimental Set-Up Concept

$$V^2 = U^2 + 2gH \tag{2.1}$$

where V is the final velocity, U is the initial velocity, g is the acceleration due to gravity and H is the height.

Force signals from the test hammer and load cells were simultaneously collected via a fast response data acquisition system which were linked to the computer running the analysis software. The software took the force over time histories and provided the Fast Fourier Transforms to provide the scrutiny of the vest. The analysis software was then planned to be programmed with the attributes to distinguish between a safe and an unsafe vest with the final output being a red flashing light for an unsafe vest and a green light for a safe one.

2.3.2 Actual VEST Experimental Set-Up

The VEST experimental arrangement was built using the following procedure. The set-up mentioned here is in reference to the second set of frames manufactured as all the validation was done using these set of frames. However in order to mention the progress in the achievement of project objectives, the set-up with the first set of frames is also mentioned in section 2.4.3.

- Two steel frames weighing 22 lbs each with a circular cut in between and 33 holes along their edges to clamp them together with bolts had a sample sandwiched in between. The bottom frame was placed on the base fixture shown in figure 2.2(c) for alignment of the frames.

- Once the sample was clamped between the frames, the entire set up was moved and placed on 4 load cells at 2.5 in from the center of the frame with the impact point intended to be at the center of the 4 load cell locations.

- The drop tower used to replicate the hammer impact (similar phenomenon of low velocity impact with similar head geometry) was raised at a height of 2 in from the sample and dropped using gravitational force. As the drop tower was mechanically controlled, it was given an impact weight of 15.4 lbs.

- Once this apparatus was ready and connected to the computer for analysis, the drop tower was allowed to fall due to gravity on the sample while constantly monitoring the force over the time histories.

- Reaction forces were recorded at the 4 load cell locations.

- The force over Time Histories were then converted to Fast Fourier Transforms to study their behaviour.

The current testing procedure involves the destructive testing of the body armor by strapping it to a support and shooting bullets through the jacket as shown in figure 1.5 The proposed experimental set-up for the corresponding non-destructive

evaluation is shown in figure **??**. These figures show the different aspects of the experimental set-up including parts like flatteners whch are not directly involved in the process to the software set-up.

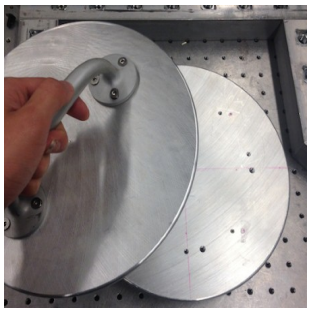

(a) Upper and Base flattener

(b) Drop tower mechanism

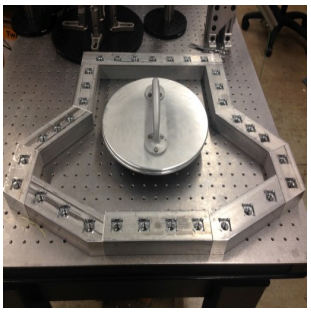

(c) Base fixture for the alignment of the frames

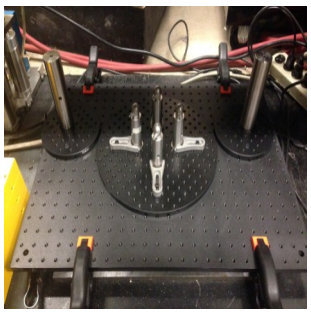

(d) Load cell arrangement

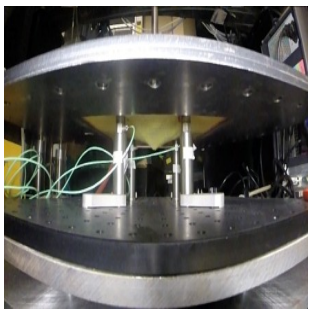

(e) Side view of Load cell arrangement

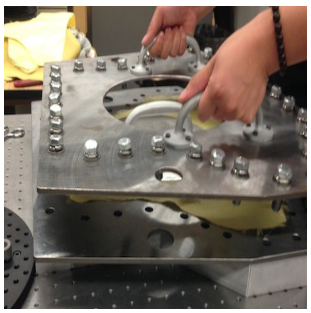

(f) Placement of top and bottom frames

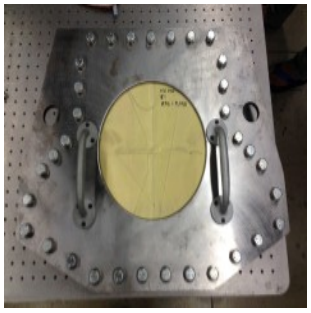

(g) Top view of the Frame set-up

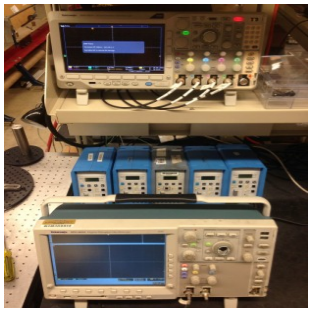

(h) Computer Analysis arrangement

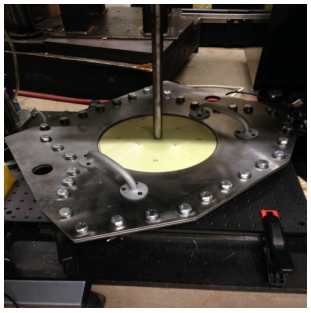

(i) Arrangement with the impactor

Figure 2.2.: VEST Experiment

2.4 Finite Element Validation of the Experiment

As the simulation analyst, the main task needed to be completed was to build a Finite Element model to physically and conceptually replicate the experimental procedure which could be used to validate the VEST set-up. ABAQUS Explicit version 6.14 was used in order to carry out the hammer impact simulations involving a low velocity impact. However, the development of the model was a progressive attempt mentioned in the following section.

2.4.1 Attempts to correct the Simulation

This section gives a basic introduction to the history of development of the Finite Element Model in terms of its accuracy to duplicate the experimental set-up in ABAQUS.

Simulation with the initial frame geometry

This assembly is called the Model 1 for simplification purposes. This was the first design used in the experimental set-up which was run with the two step analysis as mentioned before. This process included a set of frames initially built having a geometry similar to the vest shape. The frames were confined to move only in z direction as the initial estimate of movement of the frames in the actual experiment. Without the use of this boundary condition, the four load cells provided different values of force histories due to lack of symmetry. This was the first attempt to build a Finite Element model and replicate the experiment. After studying the initial experiments, the frame geometry and the simulation parameters were changed to increase the accuracy of results.

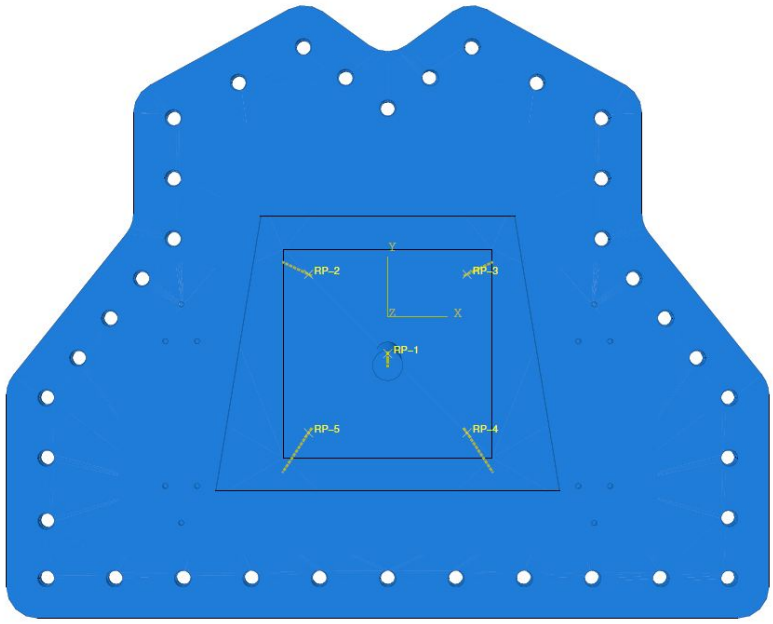

(a) Model 1 Assembly in ABAQUS Top View

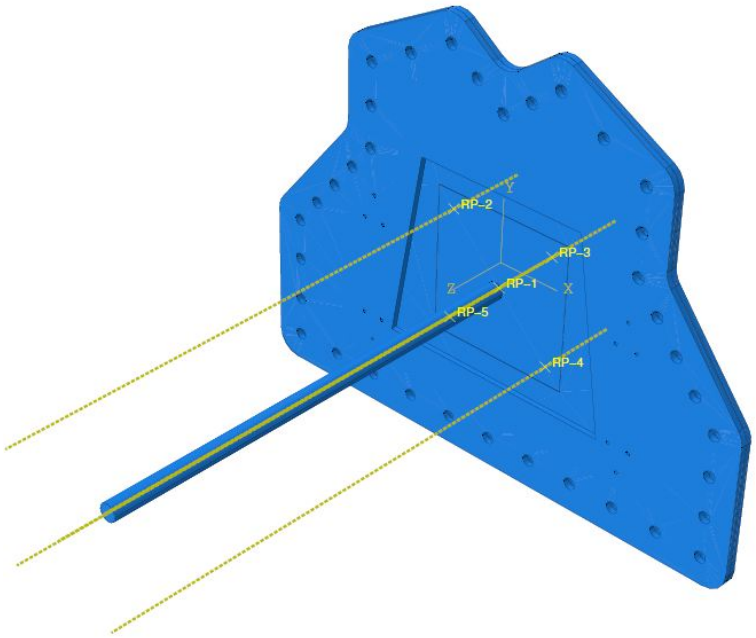

(b) Model 1 Assembly in ABAQUS Isometric View

Figure 2.3.: Model 1 Assembly in ABAQUS

Change in Simulation Parameters with the Same Frames - 3 Step Analysis

For the simplification of the naming convention this assembly was called as the Model 2. From the Model 1 analysis, it was seen that there were disturbances in the force over Time Histories. These disturbances showed after study, that they were due to the interference between the impact reaction and self weight vibrations of the frames. In order to negate this effect, the analysis was turned into a 3 step analysis with the second step taking care of the vibrations and a third step where the impactor hits a still frame preventing any kind of noise. The frames were allowed to move only in the Z direction as that was how the frames seemed to move in the experiment. During this simulation, the second step is run till the time when the frames come to a complete standstill after which the impact step is initiated.

Change in the Assembly with Same Process Parameters

This set-up is named as the Model 3 to make it easier to refer this assembly in the future topics. After the initial asymmetric plate, studies showed the need for symmetric frames to provide repeatability in results. This led to the development and manufacture of a new set of frames. These set of frames were designed in a way to keep the geometry similar to the vest geometry while trying to make the frames symmetric about X and Y direction. After the initial simulations, the frames were allowed to move in all directions to capture the actual behavior of the frames as in case of the experiment.

Validation of the Model 3

Once the Model 3 was considered to be finalized to carry out the analysis based on capturing all the concepts of the experiment, the next steps after evaluating the range of force values, included the validation of the repeatability, robustness, and the effectiveness of this set-up. This resulted in carrying out a few simulations in

order to test these above mentioned properties. This was an attempt to provide an improvement in the experimental set-up helping towards the ultimate goal of providing an accurate testing method.

Updated Model after Validation of Model 3

After the validation of the experimental set-up using Finite Element Analysis, a few issues were found with the existing process parameters related to the moving frames, position of the load cells as well as the geometry and weight of the frame which indicated the need to opt for a change in the parameters, geometry and the concept of the experimental set-up and its corresponding Finite Element Model. This finally led to the new arrangement which will be explained in the current work section. This set-up was named as the Model 4 for referral purposes.

Table 2.1 shows the history of development of models with their process parameters.

Table 2.1.: History of Finite Element Models Used

Model	Geometry	Parameters	Boundary on Frames
Model 1	Trapezoidal Geometry matching vest geometry	2 step analysis with default and impact step	Frames allowed to move in Z direction only
Model 2	Same geometry as model 1	3 step analysis with default, self weight vibration and impact step	Frames allowed to move in Z direction only
Model 3	Simplified geometry resembling a quadrilateral	3 step analysis with default, self weight vibration and impact step	Frames allowed to move in Z direction as well as Frames allowed to move Freely
Model 4	Square Shaped Frames	2 step analysis with default and impact step	Bottom frame encastered while top frame pushed down with 105 lbf at 4 locations

Owing towards the accomplishment of setting up this model, the entire Finite Element Set-Up is mentioned in the following section.

2.4.2 Individual Parts

The entire set-up consisted of 5 main parts assembled together to duplicate the VEST experiment. These five parts included:

- Top Frame
- Bottom Frame
- sample
- Impactor
- 4 Load Cells

There parts once modelled in the part module were then assembled to carry out the required analysis.

Top and Bottom Frame: These two frames had the same geometry, made out of the steel with a young's modulus of 210 Gpa and a Poisson's ratio of 0.3. The trapezoidal shaped frame geometries were designed in CATIA V5 and imported into ABAQUS. These frames had a circular cut section of 5 in radius which formed the test section area. The mesh on this part had Linear type elements used specially for Explicit simulations. These parts were given a free mesh with tetrahedral elements C3D4 of size 15mm length due to complex geometry . The mesh did not appear to be too fine, however the frames did not affect the simulation apart from the influence of their self-weight which was taken care off by assigning the weight to a reference point at the centre of mass of the frames. In order to reduce the time for simulation, the frames were made rigid bodies after being assembled. The element size of 15 mm was selected after running a few test simulations such that these elements were not

too coarse to alter the geometry. These frames were then assembled with the sample in between them.

Sample: The sample used had the same properties as the frames with Young's modulus being 210 GPa and its Poisson's ratio being 0.3. The sample was designed to shape like the outline of a vest which was more or less trapezoidal in shape. The mesh on the steel had Linear type elements used specially for Explicit simulations. Since the geometry of the sample was relatively simpler, a swept mesh was used on the sample with hexahedral elements C3D8R. The circular partition on the plate, which was directly impacted by the impactor, had a finer mesh with element size of 2 mm and the outer portion had same hexahedral elements of size 5 mm. The sample was aligned with the frames such that the center of mass of the plate and frame were coincident. The mesh size for the circular section was considered 2 mm as it gave a fairly accurate result in relatively lesser time after studying the results from varying element sizes from 1 mm to 5 mm.

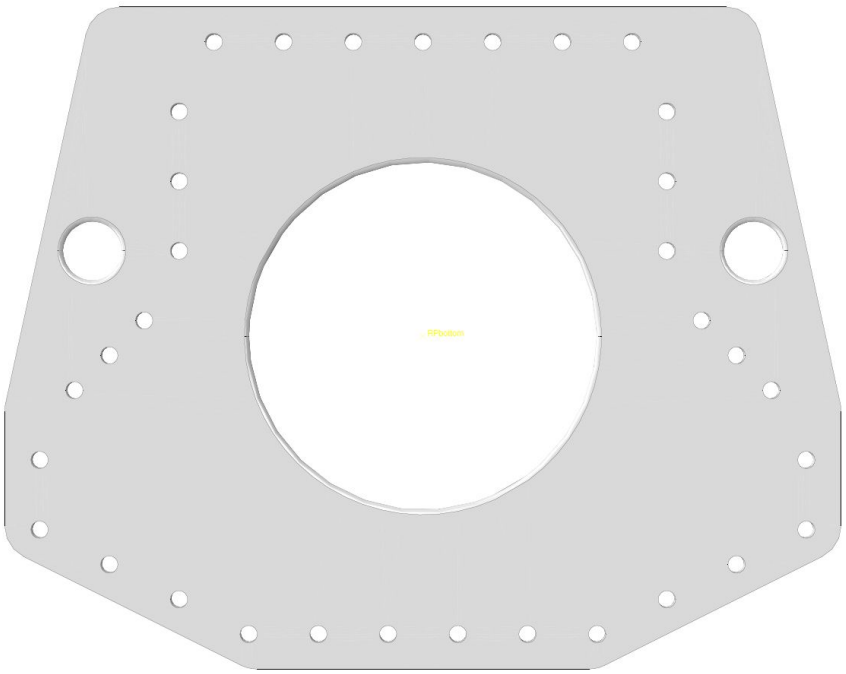

(a) Top/Bottom Frame Geometry

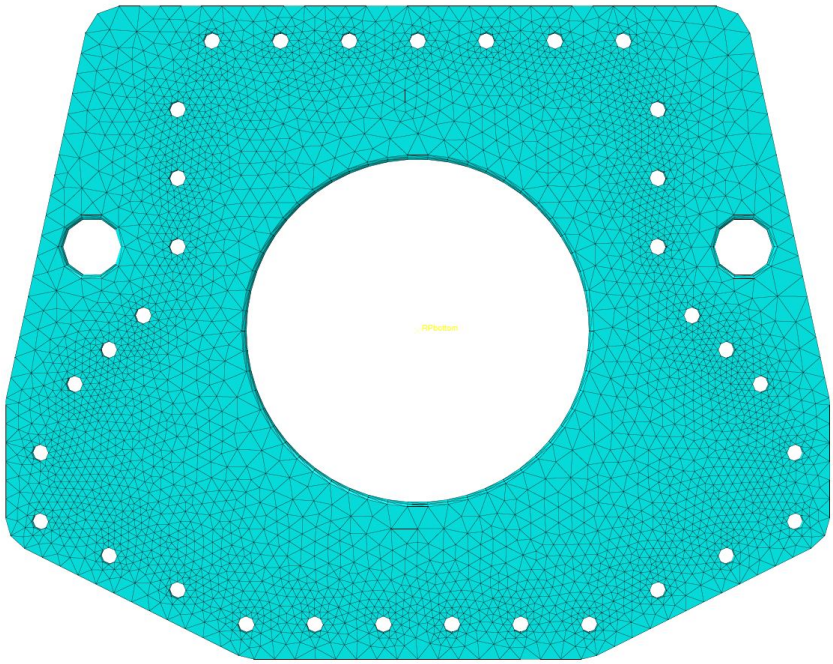

(b) Top/Bottom Frame Mesh

Figure 2.4.: Top and Bottom Frame

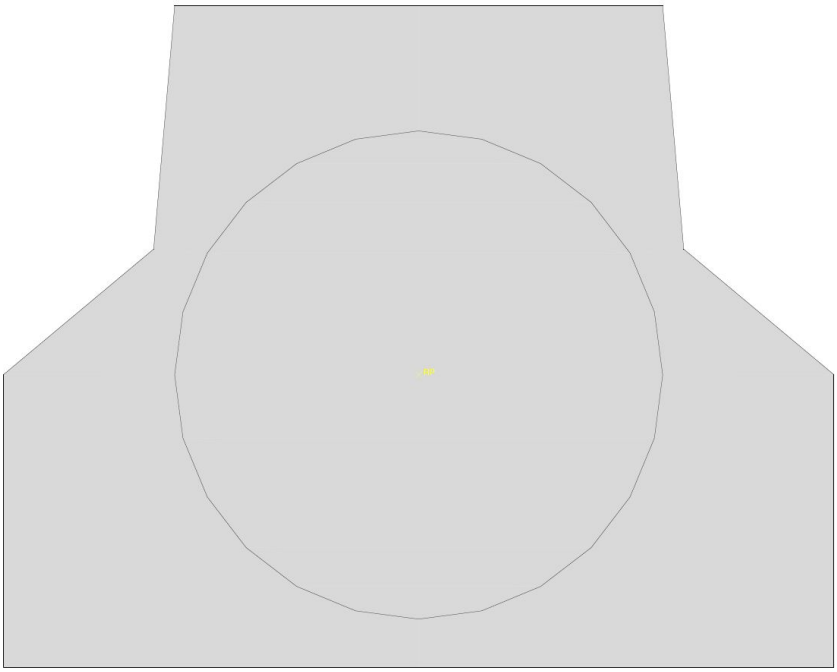

(a) sample Geometry

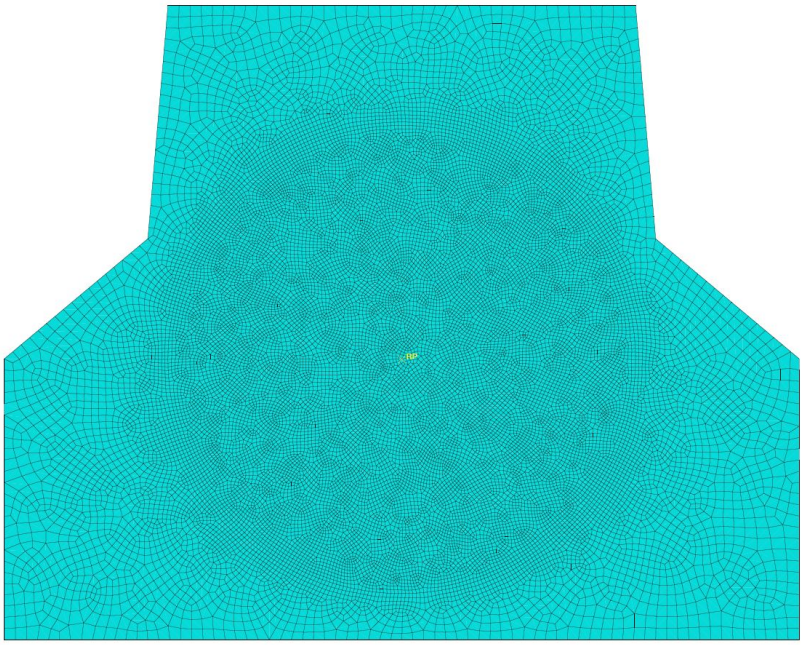

(b) sample Mesh

Figure 2.5.: sample

Impactor: The impactor was a cylindrical shaped part with a half sphere at the end that impacts the sample. The impactor was connected to the mechanical drop tower in the experiment. In ABAQUS the impactor was modelled as an analytical rigid body. The analytical rigid body saved the computational time due to lack of need for meshing. The fact that the experiment was carried out in the elastic region, the analytic rigid body did not change the dynamics of the experiment. Since the actual experiment had a mechanism to input a dummy weight to the system, a weight of 15.4 lbs was attached to the reference point of the impactor.

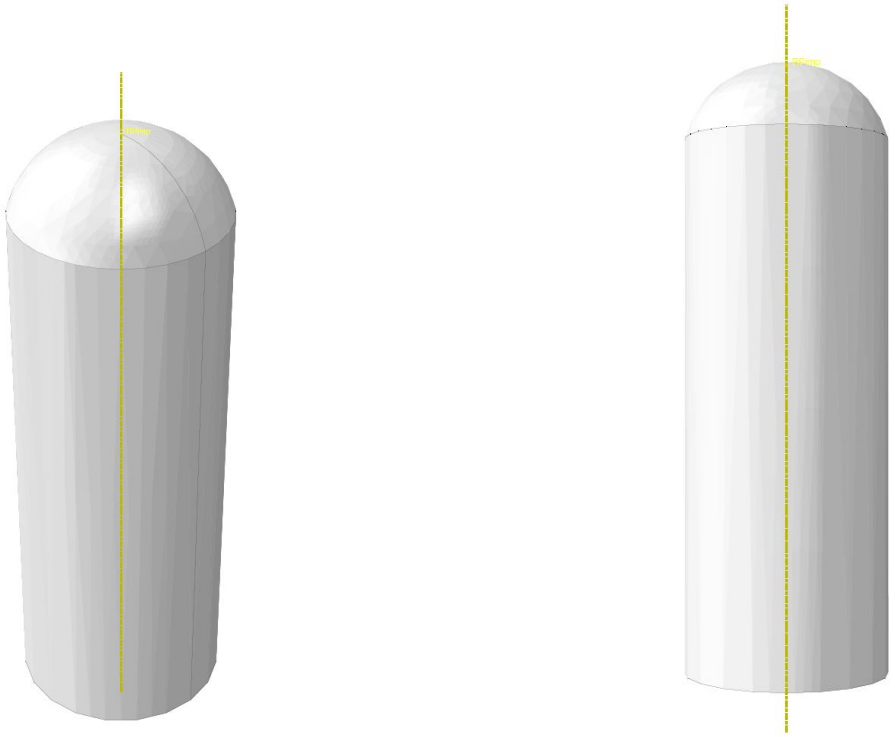

(a) Impactor Geometry

(b) Impactor Front View

Figure 2.6.: Impactor

Load Cells: The load cells were made of steel with the same properties as the frames and the plate. These load cells used a mesh with hexahedral elements with element size of 2 mm. It was seen that the element size of 2 mm was fine enough to provide accurate results based on sensitivity study. 4 such load cells were used in the set-up placing the frame and plate arrangement on the load cells.

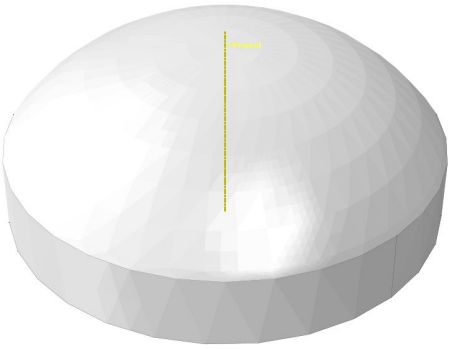

(a) Load Cell Geometry

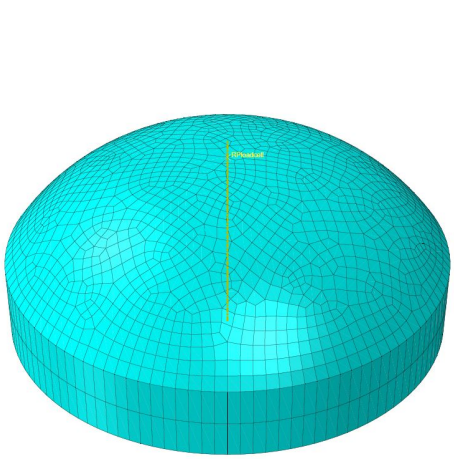

(b) Load Cell Mesh

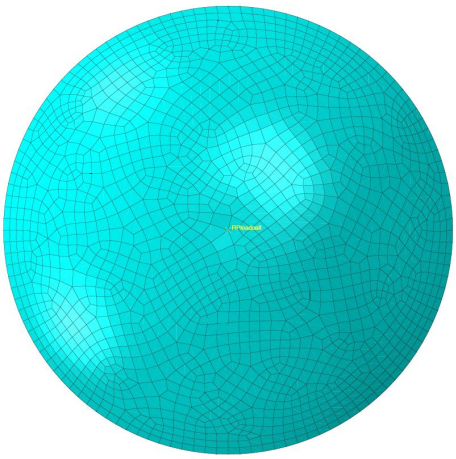

(c) Load Cell Mesh Top View

Figure 2.7.: Load Cell

2.4.3 Finite Element Model Arrangement

Finite Element Step by Step Procedure

Once these individual parts were modelled in the Part Module of ABAQUS, they were then assembled in the Assembly Module and assigned the required properties to resemble the actual experiment.

Assembly: The sample was first aligned with the reference point at its center of mass at coordinates 0,0,0 (origin). Once the sample was assembled, the top and bottom frames were assembled such that the reference points at the center of mass of the frames were aligned along the z axis with the same x and y coordinates of 0,0. Next, the load cell was imported in the assembly 4 times so that these 4 load cells were arranged at 2.5 in from the center of mass of the plate at 45 and -45 degree line such that these load cells were just in contact with the plate. Finally the impactor was aligned along the z axis at 2 in above the origin with its spherical section facing the plate making the apparatus ready to be assigned test properties.

Step: Initially the experiment was set-up with a 2 step analysis with the default initial step and a dynamic-explicit step. After a few simulations and initial changes, the set-up was changed to a 3 step analysis with a default initial step, a dynamic-explicit step for vibrations due to self weight and another dynamic-explicit step for the impactor to hit the plate.

History Output: The reaction forces were noted at the bottom surface of the load cells. The history output was requested for all 4 load cells at 200 time intervals in 2nd step (vibration step) as the smoothness of that plot was not that important. On the other hand the force histories were recorded at 10000 time intervals to obtain an accurate behavior at the load cell locations.

Interaction: A tangential behavior interaction was used for the experiment with a friction coefficient of 0.5 as it is the frictional coefficient generally used for steel to steel interactions.

Constraints: Four main constraints were involved in this set-up. The top and bottom frames were made rigid while the top and bottom frames were tied to the sample with the surfaces in contact.

Load: There was only 1 load involved in the simulation where the impactor was allowed to free fall using gravity.

Boundary Conditions: There are two main boundary conditions included in these simulations. The load cells were encastered as they did not move at all during the course of the analysis. On the other hand the impactor was allowed to move only in the z direction as the drop tower moves only vertically downwards. In certain simulations carried out before finalizing these boundary conditions, an added condition included allowing the frames to move only in the Z direction. However it was later found out from the experiment that there were lateral movements in the frames that led to the removal of this boundary condition letting the frames move freely.

Job: Once these settings are input, the job is submitted with 16 cores as that was the maximum allowable cores on the system used. More number of cores helped to reduce the computational time as compared to just one core.

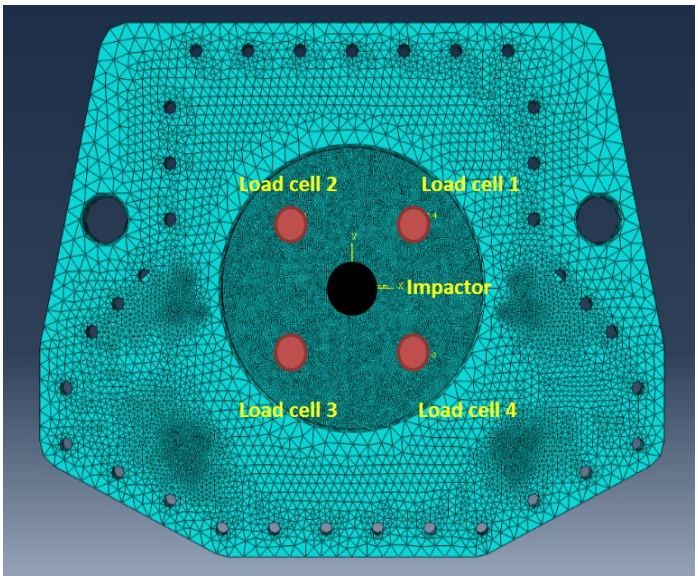

(a) Experiment Assembly in ABAQUS Top View

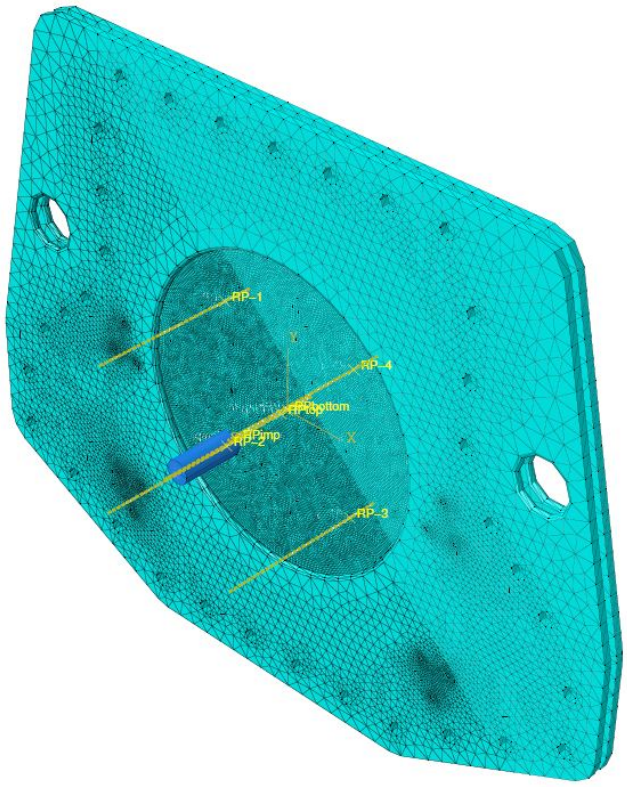

(b) Experiment Assembly in ABAQUS Isometric View

Figure 2.8.: Experiment Assembly in ABAQUS

3. Results and Discussion

3.1 Initial Results

This section talks about the results of the simulations carried out on the first couple of frames set-up. They include all the simulation runs before carrying out the validation.

3.1.1 Model 1 Results

The initial simulation involved a two step analysis with the default Initial step and then the Dynamic-explicit step. The simulation was run for 0.15 s based on a few try runs to finalize on this time. Once the simulation was completed, the force over time histories were plotted.

Figure 3.1 shows the response of the load cells to the impactor hitting on the sample. In this figure, it is seen that the graph shows a small disturbance just before 0.02 s at about 50 lbf of amplitude. After a careful study of this phenomenon, it was observed that this disturbance was due to the interference of the impactor hitting the sample with the movement of the plate due to the vibrations of the frames lying on the load cell unconstrained. This was one of the main conceptual difference between the experimental set-up and the Finite Element Analysis.

In the actual experiment, the clamped frame arrangement was carefully placed on the 4 load cells. Once the alignment was corrected and the frames settled on the load cells, the set-up was ready to carry out the analysis. However, in ABAQUS, as the arrangement was placed on the load cells, it did not show any disturbance till the job was run.

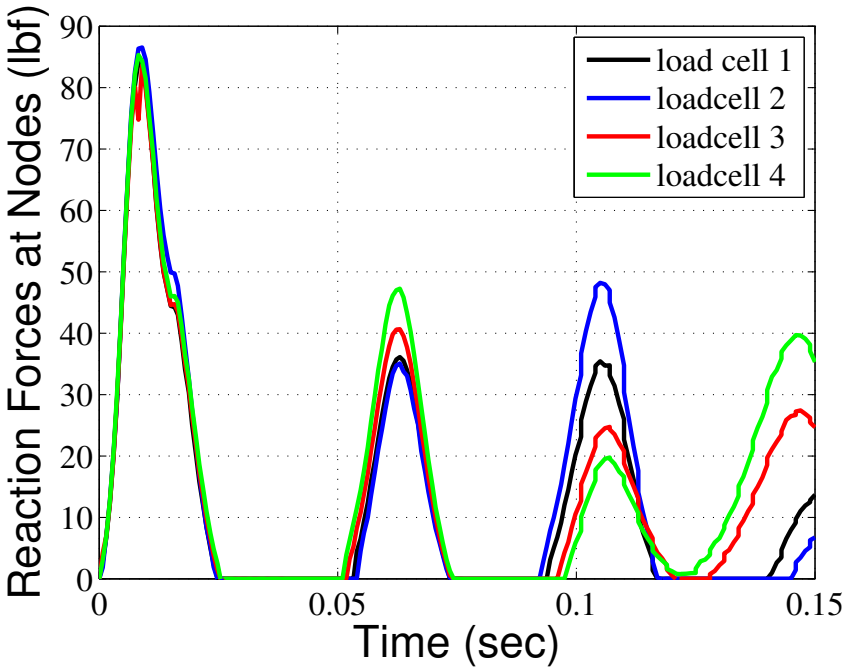

Figure 3.1.: Model 1 Plot for Force Over Time

Once the job was submitted, the software considered a weight of about 44 lbf suddenly dropped on the load cells leading to vibrations due to self weight. This suggested a need to take into account these vibrations in the simulations which led to the first modification in the simulation which involved a change in process parameters related to the analysis steps. Appendix B shows the simulation with the same set-up for 0.5 m/s velocity. This figure also suggests the same issue related to the disturbances.

3.1.2 Model 2 Results

After spotting the issues with the Model 1 leading to inaccuracy, it was necessary to take these vibrations into account for which the simulation was changed to a 3 step analysis. After the first default initial step, the second step involved letting the frame vibrate due to its own weight. This step ran for one second after realizing it

took about that much time for the frame to come to a standstill. The third step was finally the impact step for the same amount of time i.e. 0.3 seconds. These step times were decided based on trial simulations the cover the entire process dynamics.

Figure 3.2 shows the effect of reaction forces on the bottom surface of the plate and the bottom surfaces of the load cells where the reaction forces are studied.

This figure shows how the bottom surface of the plates and the load cells look as the set-up experiences vibrations due to movement of the frames.

Figure 5.8(a) shows the plots for the analysis carried out with the frames moving only in the Z direction due to impact as well as vibrations. It took about 1 second for the frames to come to a standstill. From these figures, we can see that the simulation starts from about 10 lbf on each load cell rather than zero. This is due to the weight of the frames being around 40 lbf. Figure 5.8(b) shows the third step of the simulation to give a better picture of the impact step. Due to the boundary conditions on the frames the forces are almost the same on all the load cells. However, the experimental set-up recorded different values at different load cells that made it necessary to change the frames geometrically.

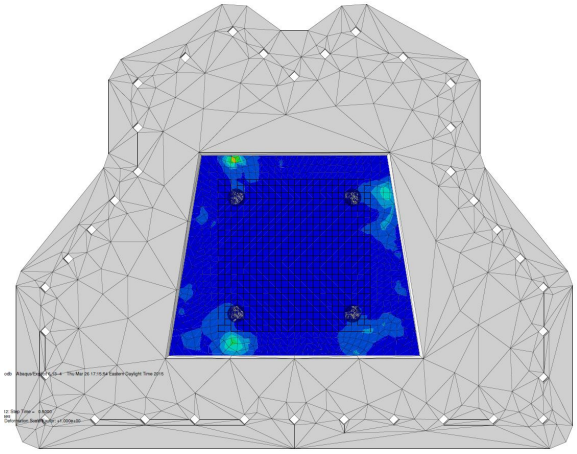

(a) Effect of Vibration on the Bottom Surface of the Plate

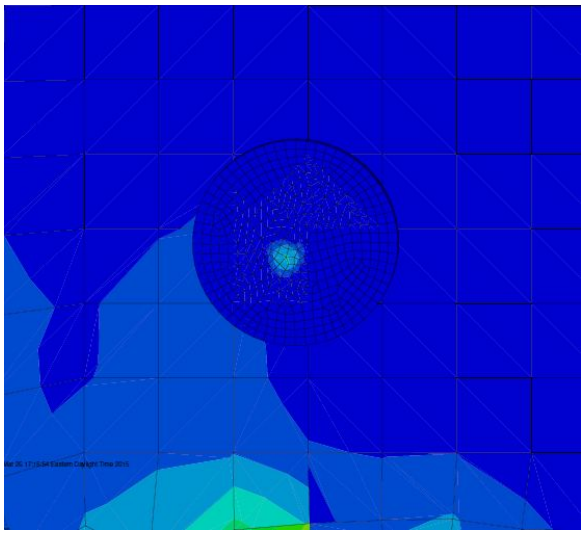

(b) Effect of Vibration on the Bottom Surface of the Load Cell

Figure 3.2.: Effect of Vibration

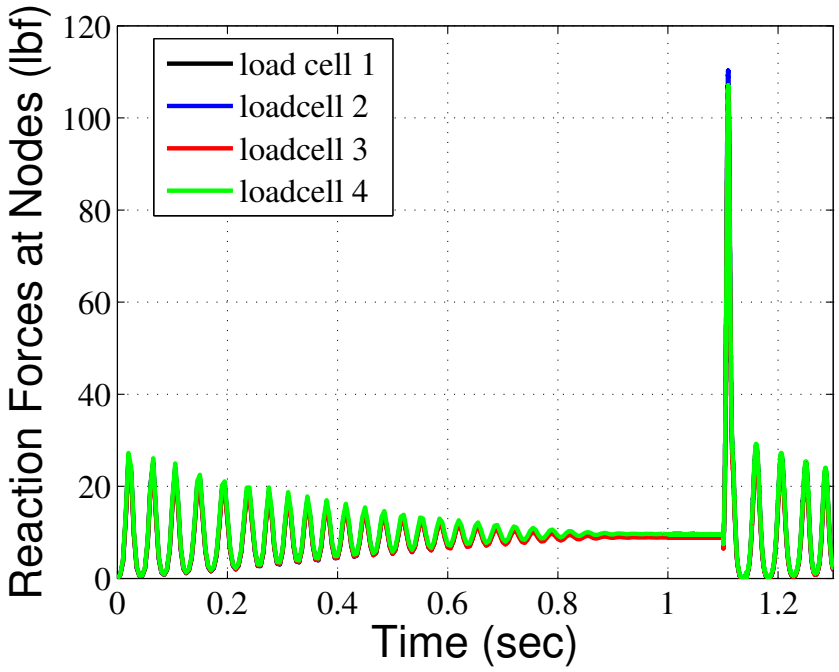

(a) Model 2 Plot for Force Over Time

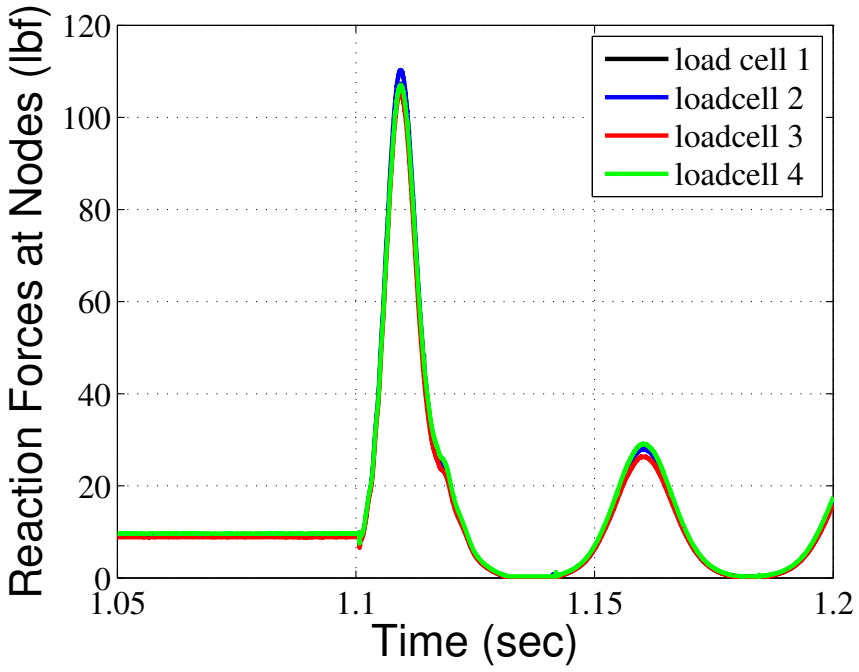

(b) Model 2 Plot (Step 3) for Force Over Time

Figure 3.3.: Model 2 Plots

3.1.3 Model 3 Results

After a few initial experiments, the lack of symmetry raised the questions related to the accuracy of the experiments. The geometry of the frame was finally changed in an attempt to bring the center of mass and center of geometry of the frame as close as possible. While doing this, the frame geometry was mode somewhat quadrilateral still covering the entire vest dimensions. This update was made in an attempt to improvise the overall symmetry of the set up to result in equal reaction forces at all load cell locations. This set-up is the same one as mentioned in section 2.4.3.

Simulations were run with and without constrained frames with this set-up. Figure 3.4 shows the simulations with constrained frames. These figures follow the same trend in behavior as figures 3.3. Only difference is the fact that the maximum force recorded at every load cell dropped from about 114 lbf to about 107 lbf with the change in frame geometry even though the time take for the peak to subside was almost the same. Considering an increase in frame weight should have increased the maximum recorded values, it was realized that the constrained frames provided inaccurate results.

After validating the fact that the maximum forces dropped instead of increasing, the constraint on the frames is removed and the frames were allowed to vibrate freely. This was mainly because, it was seen from the experiment, that these frames moved laterally by some small margin as they vibrated due to self weight. In order to prevent them from totally slipping, the required coefficient of friction of 0.5 was entered (steel to steel frictional coefficient) and the parameters involved were the ones mentioned in the Method section. Figure 3.5(a) shows the entire simulation results and figure 3.5(b) shows the third step of the simulation. Figure 3.5(b) shows a similar force at locations 3 and 4 which was about 116 lbf and also at locations 1 and 2 which was about 108 lbf. This was expected as the load cells are along the diagonals from the center shown in figure 2.8(a) with locations 1 and 2 on the top half, while locations 3 and 4 in the bottom half. Due to this, the two sets of locations have a slightly different force which

was also encountered in the experiment. Further, the plot shows values going to 0 lbf between the peaks even though the frame weight is about 44 lbf. This was mainly because the frames lost contact with the load cells and sprung up due to sudden impact.

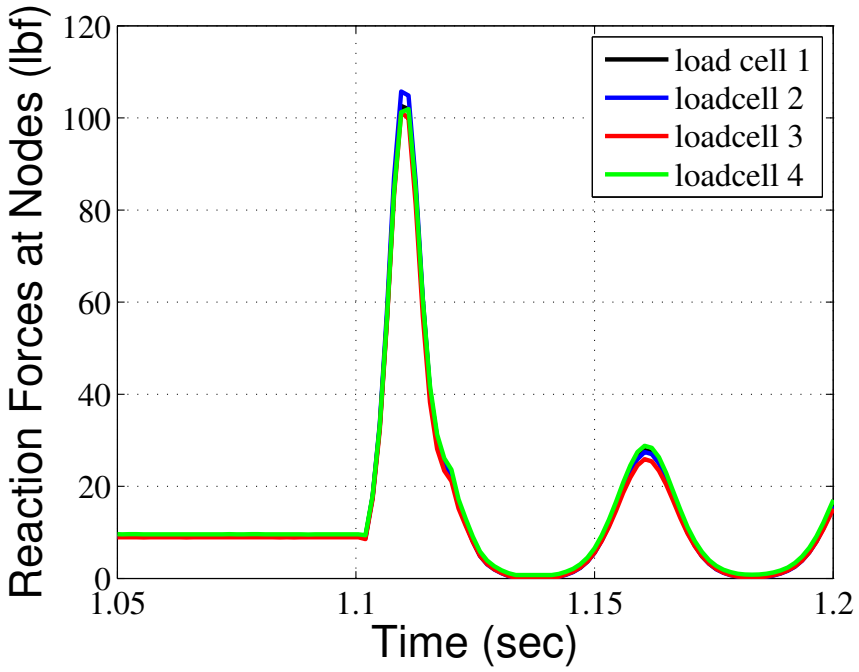

(a) Model 3 Plot with Constrained Boundary Conditions

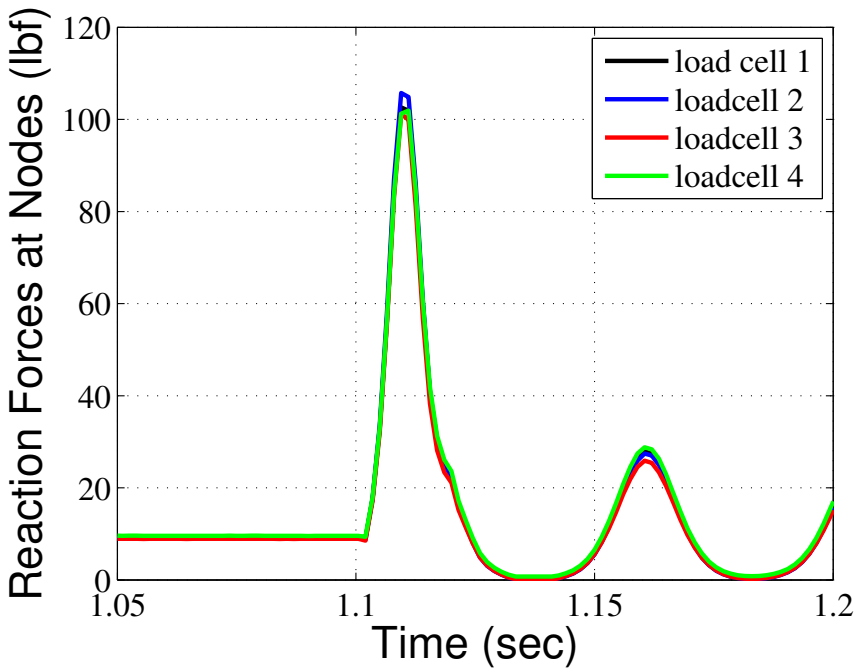

(b) Step 3 of Model 3 Plot with Constrained Boundary Conditions

Figure 3.4.: Model 3 Simulation with Constrained Frames

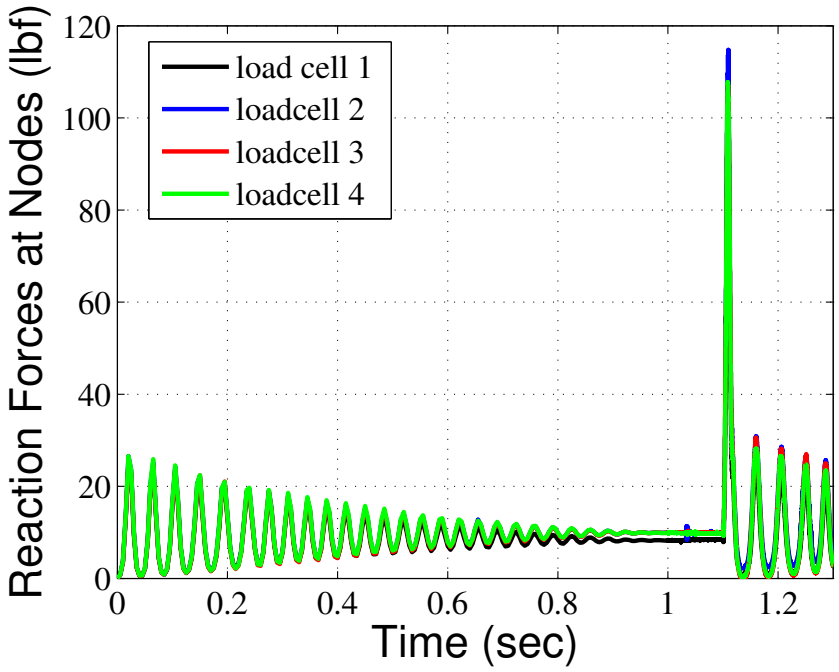

(a) Study of Model 3 with No Boundary Conditions

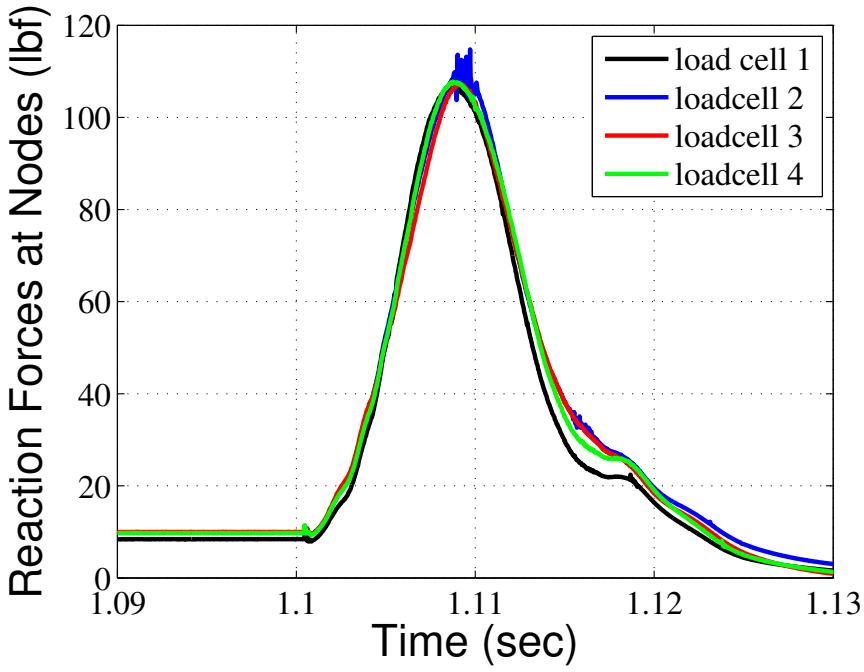

(b) Step 3 of Study of Model 3 with No Boundary Conditions

Figure 3.5.: Model 3 Simulation with No Boundary Conditions on Frames

3.2 Validation

Even though the simulations showed force values following a behavior similar to that suggested by the theories, the actual experiments had erratic results, non repeatable, and inaccurate results every time the experimental analysis was carried out. This led to a need for validation which is spoken about in this section testing different properties of the model.

During the validation phase, the first peak of force over time after impact was chosen to be the region of study. The secondary peaks were disregarded as they were basically due to multiple impacts and vibrations. A set of simulations were run with an attempt to study different issues with this set-up to provide improvisations if any. The load cell locations were changed from being arranged diagonally from the center to directly along the x and y axes from the center at 2.5 in in the experimental set-up.

These simulations were incorporated with these changes and the experimental set-up validation was carried out to determine its effectiveness.

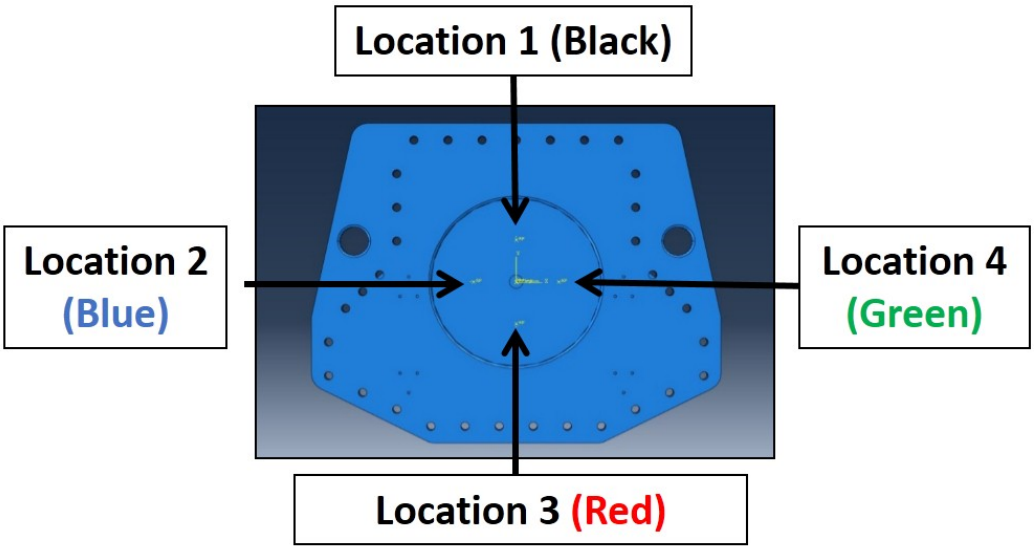

Figure 3.6.: New Load Cell Locations

3.2.1 Variations in Different Load Cell Location Readings

The frames used in this set-up are seen in figure 3.6 with the corresponding load cell locations seen from the top surface. Even though the impact was made at the center of mass, the simulation results shown in figure 3.7 show different values of force at different load cell locations.

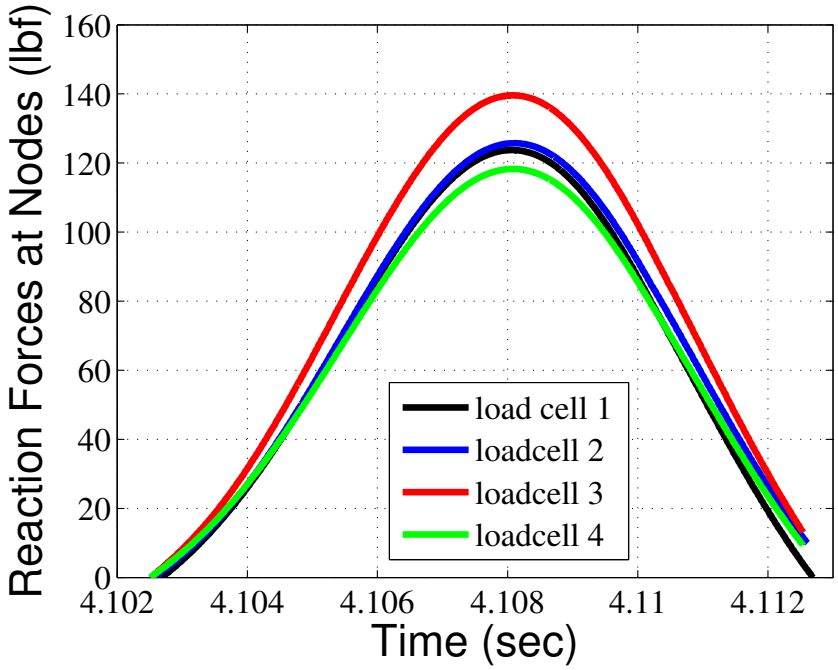

Figure 3.7.: Load Cell Force Response for the New Frame on a sample

The frame seen in figure 3.6 was built in such a way that the center of mass and center of geometry coincided. However, there were two main factors that influenced the difference in results. First, the frames were symmetric about the y axis, but there was no symmetry about the x-axis. The second issue was the fact that the load cells were equidistant from the center leading to different moment of inertia on load cells 1 and 3. Due to these two factors, the impact led to a variable amount of force on the load cells 1 and 3 while the reaction forces remain more or less similar on load cells 2 and 4 if not exactly same.

This was validated by the huge difference in values in the red and black graph which belong to locations 1 and 3 respectively. Ideally the force values recorded at load cell locations 2 and 4 should have been very close to each other if not same. In this simulation, the values were relatively close however not exactly the same due to mesh effects, effect of friction, and moving of the plate slightly due to vibrations of these frames due to self weight in presence of friction. This led to the movement of the frames from its positions laterally before moving to the impact step in the simulation. It was seen that the frame set-up moved about 2 mm in the z direction towards the bottom end of the frame tilting the frame, about 0.5 mm in the Y direction towards location 3 and about 1 mm towards location 2 in the X direction. Despite the presence of friction, the frictional coefficient of 0.5 was not enough to hold the frames at their position during vibrations. These movements in the frame lead to the difference in force values at all four load cell locations.

3.2.2 Analyses to Compare Different Materials

In order to verify this fact and to study the effect of different materials, a few simulations were run with materials with smaller Young's moduli, properties of Kevlar fiber as well as a hypothetical fabric with properties listed below:

This was an attempt to study the behavior of different materials based on their Young's moduli. However, the variation in the forces captured at load cell locations in figure 3.7 on a sample analysis, followed the same trend with all the materials shown in the table 3.1 which can be seen from figures 3.8 and 3.9

Table 3.1.: Material Used for Analysis

Material	E1 (GPa)	E2 (GPa)	E3 (GPa)	v12	v23	v13	G12 (GPa)	G23 (GPa)	G13 (GPa)
Material 1 (Isotropic)	210	210	210	0.3	0.3	0.3	-	-	-
Material 2 (Isotropic)	100	100	100	0.3	0.3	0.3	-	-	-
Material 3 (Isotropic)	84.62	84.62	84.62	0.3	0.3	0.3	-	-	-
Kevlar Fiber [19]	84.62	1.34	1.34	0.24	0.6	0.24	24.4	0.42	24.4
Fabric	100	100	40	0.24	0.6	0.24	10	5	10

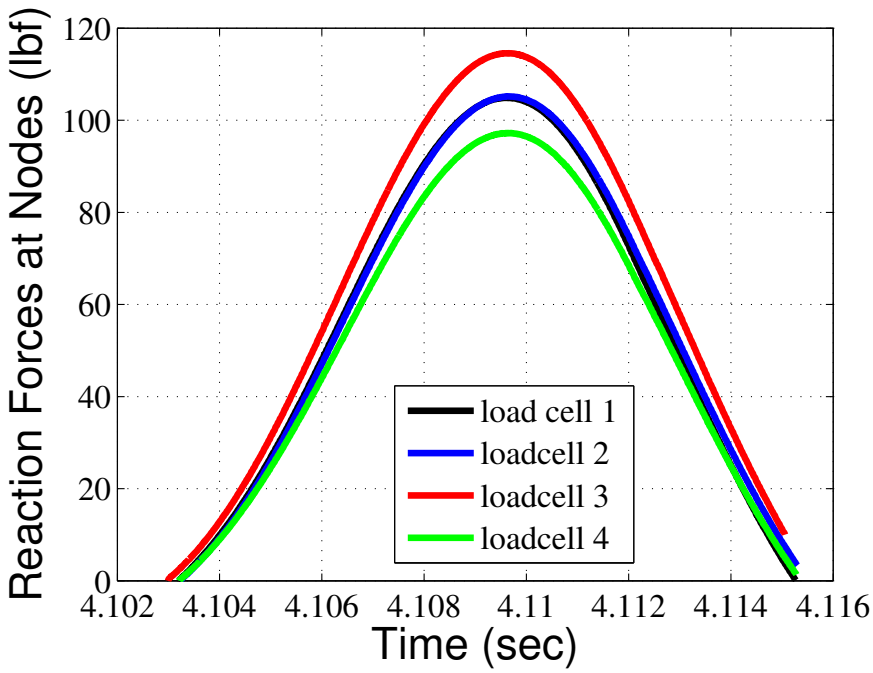

(a) Load Cell Force Response on an Isotropic Material with 100 GPa Young's Modulus - Material 2

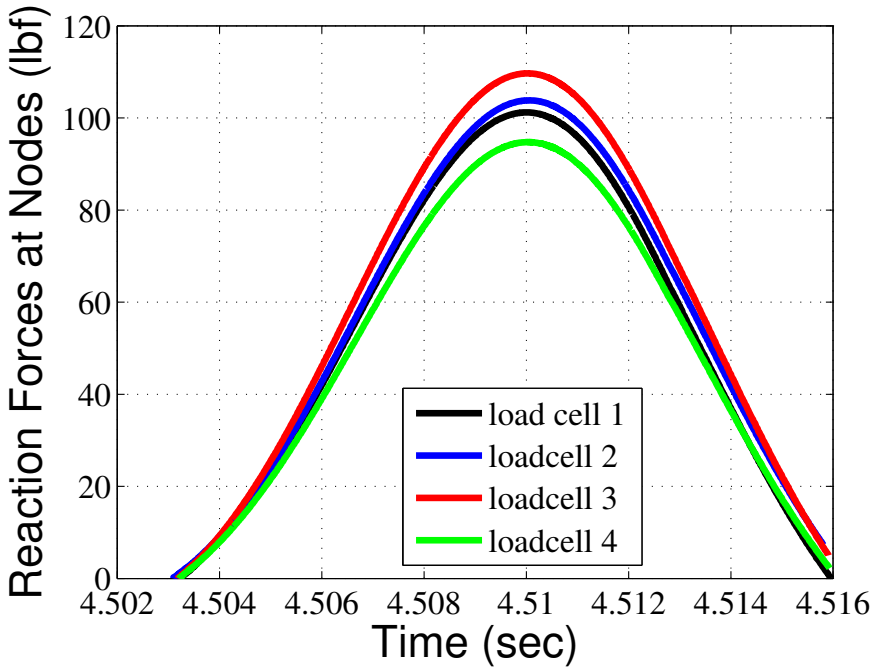

(b) Load Cell Force Response on an Isotropic Material with 84.62 GPa Young's Modulus - Material 3

Figure 3.8.: Model 3 Simulation for Isotropic Materials

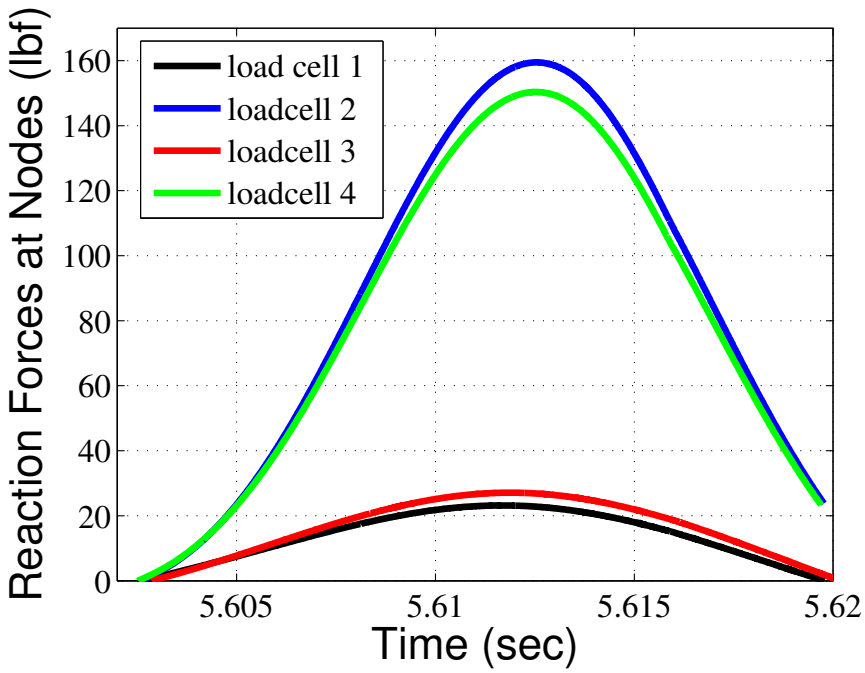

(a) Load Cell Force Response on a Homogeneous Material With Kevlar Fiber Properties - Kevlar Matrial

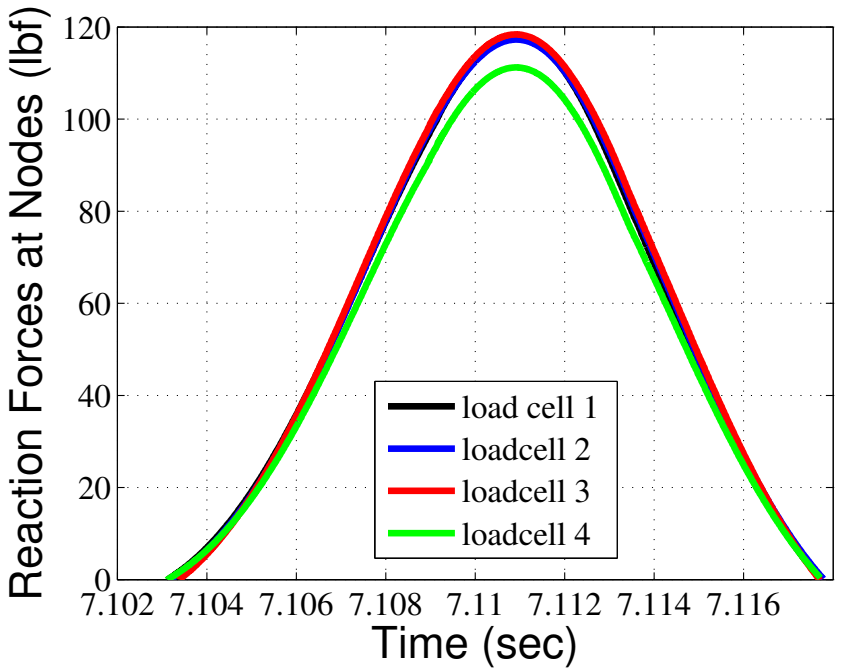

(b) Load Cell Force Response on a Fabric

Figure 3.9.: Model 3 Simulation for Isotropic Materials

- Figures 3.8(a) and 3.8(b) showed the simulations for isotropic materials 1 and 2 respectively. These figures display equidistant reaction force values between load cell locations 1 and 3 as well as locations 2 and 4. A phenomenon that was not noticed in the simulation with sample. This particular response was not the actual expected one as ideally, the values at locations 2 and 4 should have been the same. This difference was again accredited to the haphazard motion of the frames during vibration due to the frame movement mentioned previously in section 3.2.1. Further, the force maximum force values differ for these two materials due to the difference in their properties. The maximum force for material 2 is about 116 lbf and that for material 3 is about 110 lbf.

- On the other hand figure 3.9(b) shows the analysis results on the fabric. Apart from load cell 4, all three other load cell locations recorded almost the same amount of reaction forces totally different from the analysis results from isotropic materials. Reason for this was same as the one mentioned above for the isotropic materials

- Further, if the simulation for the homogenized kevlar fiber material was observed, there was a vast difference between reaction forces at locations 1 and 3 and locations 2 and 4. This was expected as the fiber was very weak in the transverse direction as compared to the longitudinal direction. Hence the forces captured at locations 1 and 3 (load cells located along the transverse direction) are way smaller than that at locations 2 and 4 (load cells located along the longitudinal direction)

So few issues related to this set up were as follows:

- **Repeatability**: The vest was aligned between the frames manually and even the frame set-up was placed on the load cells manually. This involved human error leading to misalignment of the vest and frames leading to an offset from the center of mass. This was the main reason for inconsistency in the results in the experimental set-up.

The corresponding simulations mentioned above depicted the fact that movement of the frames during the vibration step led to variable impact points for every material thus reducing the accuracy and repeatability of results.

- **Load Cell Locations**: Due the the locations of load cells being directly along the x and y axes, the values for the kevlar material analysis varied to such an extent and would have not been the case if the load cell locations were along 45 and -45 degrees locations.

The actual experiment analysed the behavior of a few materials including a sample, a plastic plate, two old vests and a kevlar single ply with plain weave. This comparison graph also shows a similar inconsistent variation in the load cell values as shown in figure 3.10. All the four load cell locations for ever material recorded different values as expected due to asymmetric frames.

Similar issues being encountered with the Finite Element set-up where different values were encountered at different load cells as seen in figures 3.8 and 3.9. So, it was decided to compare the mean values of the load cell locations for comparison. Figures 3.11 shows this comparison. Sample (steel plate) took the least amount of time with maximum reaction force which was expected due to its maximum stiffness, while Kevlar followed the opposite trend. The mean of maximum force values at the load cell locations and the time taken for the completion of the impact thus bringing the peak to zero are shown in table 3.2.

The main intention of studying the effect of different materials was to evaluate if the proposed testing method would work well or not for new and aged vests of the same material. A difference in force over time histories help us determine the fact that the proposed set could be used to determine the difference between new and aged vests. Stiffness was presumed to be one of the properties to quantify ageing based on these results.

Appendix C shows the comparison between mean values of force over Time histories for same materials with load cells along the diagonals from the center and a

Table 3.2.: Comparison of Force over Time Histories for Different Materials

Material	Maximum Force (lbf)	Time Taken (s)
Sample	126.79	0.01
Material 1	105.41	0.0121
Material 2	102.33	0.0127
Kevlar Fiber	89.83	0.0172
Fabric	116.07	0.0146

boundary condition given to the frames such that the frames are allowed to move only in the Z direction. This was carried out before configuring the fact that constrained frames was not conceptually the most accurate way to set-up the frames in the simulation. Letting the frames move only in Z direction prevented the lateral movement and thus the sliding of the frames was prohibited. Due to this, the values at locations 1 and 3 very almost same, something that was initially expected to happen.

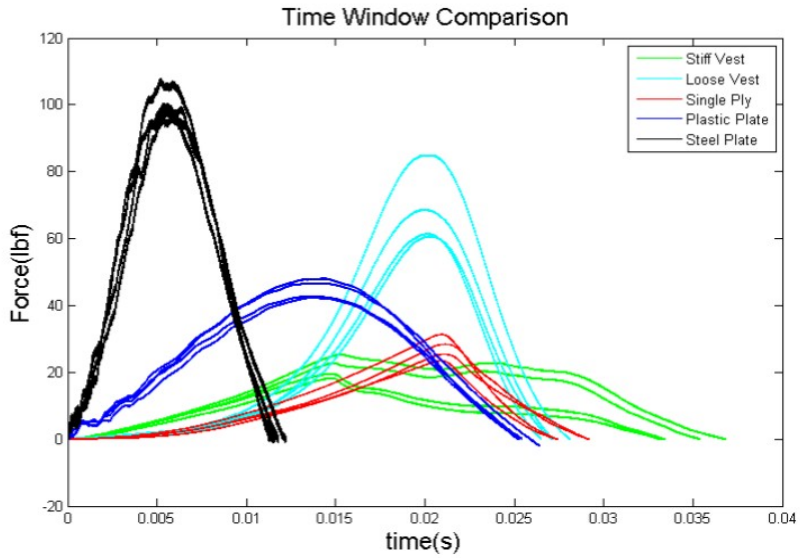

Figure 3.10.: Comparison of Different Materials through Experimental Analysis

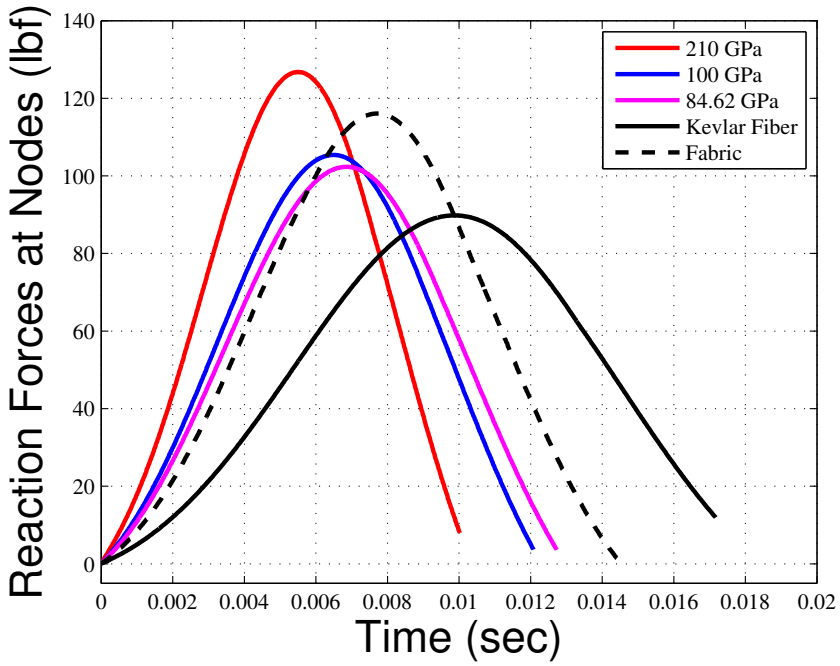

Figure 3.11.: Comparison of Different Materials through Finite Element Analysis

The Fast Fourier Transforms plot for the different materials compared is also shown in this section in figures 3.12 and 3.13. Figure 3.12 shows the basic Fast Fourier Transform plotted using the same principle as in appendix A. At frequencies above 200 Hz, all that was recorded was noise and disturbances. However at frequencies below 200 Hz, the Fast Fourier Transforms could be useful to study the behavior of different materials by noting the amplitudes at which these curves begin to normalize. The curve for kevlar is seen to normalize after a steep drop before every other material which was a result worth looking at as kevlar was the least stiff material studied. However the fact that the FFTs had an amplitude of 80 at a frequency of 0 Hz suggested the need to look at these FFTs through a different perspective.

The *detrend* function removes the mean value or linear trend from a vector or matrix, usually for FFT processing. This in turn helps to negate the dominance of 0 Hz frequency. These FFTs were then plotted with the *detrend* function shown in figure 3.13. This plot showed a firm distinction between kevlar and other materials.

Firgure 3.12 shows that the Kevlar curve normalized first at about 110 Hz followed by the fabric at 117 Hz. The curve for mild steel material normalizes the last at about 185 Hz. This shows that the normalizing of these FFTs is based on the stiffness of the materials. Further, figure 3.13 shows the FFT plot with the *detrend* function. The plot is narrowed to 100 Hz frequency in order to magnify the results. This graph also shows the same distinction where the Kevlar curve normalizes first at about 10 Hz frequency in opposition to the steel curve that normalizes at 26 Hz. However, the study of Fast Fourier Transforms was insufficient to make a solid conclusion at this stage of the project.

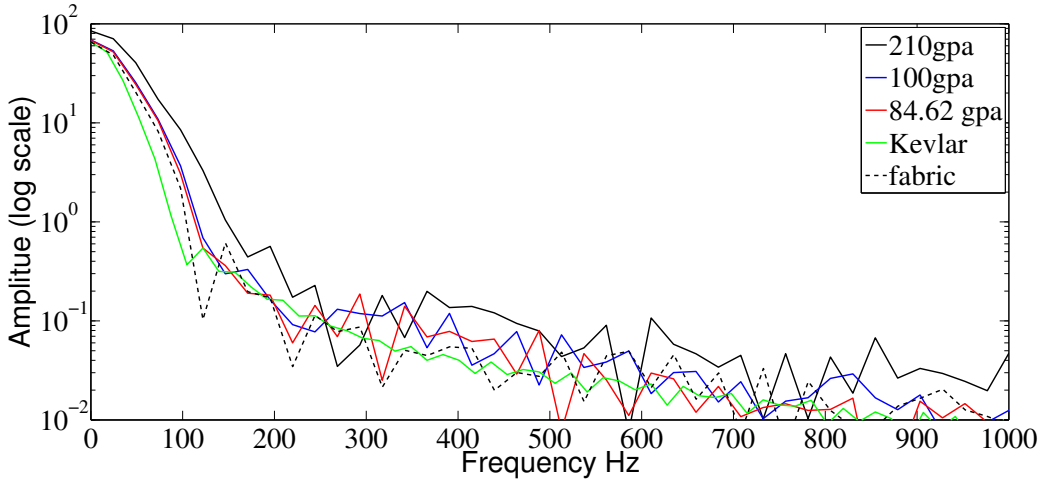

Figure 3.12.: Fast Fourier Transforms

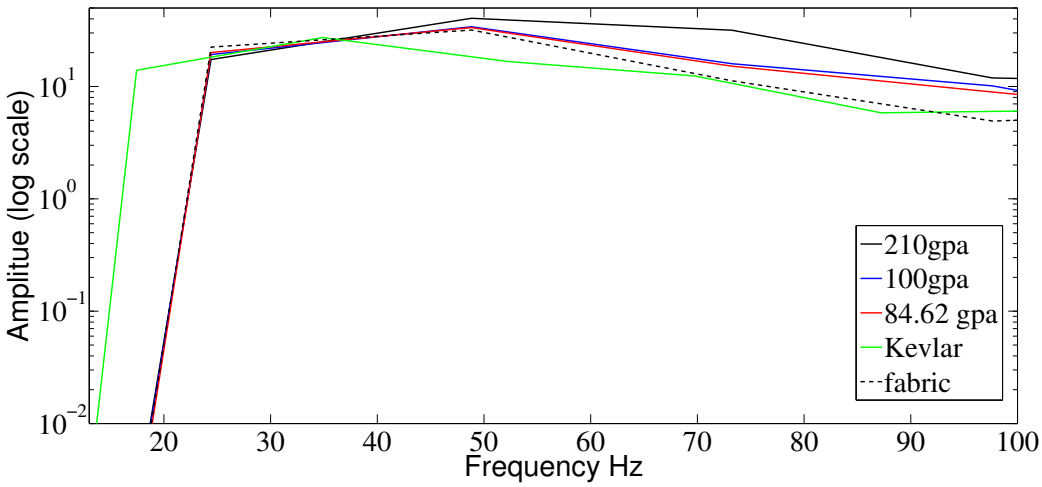

Figure 3.13.: Fast Fourier Transforms with Detrend

3.2.3 Sensitivity Analysis

Realizing the fact that the placement of the frames on the load cells in the actual experiment created quite a difference in the reactions forces at different locations, it was decided to carry out a sensitivity analysis on the impact locations to study the effect of these errors on the overall results. This difference was mainly because the frame arrangement was placed on the load cells manually which led to human error every time it was placed.

In order to establish a reference to compare with, a simulation was run with the impact happening at the center of mass of the set-up. All the parameters were kept the same for these experiments and only the impact point was varied. Figure 3.14 showed the plot for the reference simulation where the impact was made at the center of mass. This plot is the same as figure 3.7. These results were used to compare the other analyses where the drop tower was impacted at X and Y direction offsets from the center of mass.

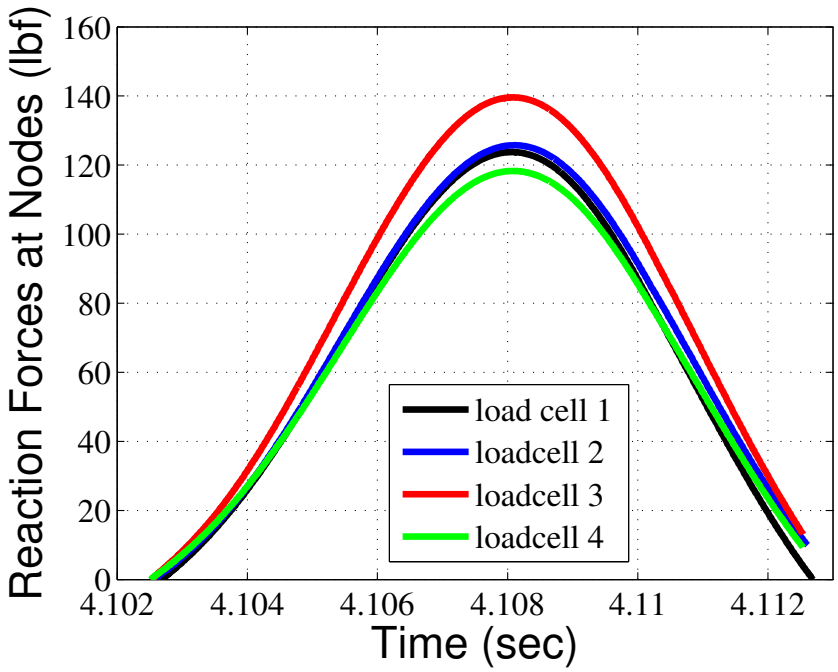

Figure 3.14.: Benchmark for Comparison - Impact at Center of Mass

In order to carry out the sensitivity analysis, the impact points were shifted with offsets of 1 mm and 5 mm in both x and y directions. Figure 3.15 depicts the analysis with offsets in X-direction while figure 3.16 depicts analysis with offsets in Y-direction.

Figure 3.15 is a representation of the impacts carried out in the X direction towards the right of the center of mass. From this figure we understand the fact that as the impact point is shifted in the X direction towards location 4, the difference between values at locations 2 and 4 keeps on increasing with an expected change where the reaction forces at location 2 goes down. There is no significant change or any pattern in the change in values at locations 1 and 3 in the Y direction during these analyses.

Figure 3.16 is a representation of the impacts carried out in the Y direction upwards from the center of mass. From this figure we understand the fact that as the impact point is shifted in the Y direction towards location 1, the difference between values at locations 1 and 3 keeps on changing. In case of the center of mass simulation, the force at location 1 is less than that at 3 as the frame is heavier in its bottom half. As the impact point is further north of the center, the reaction forces at location 1 keep on increasing and those at location 3 go on decreasing. There is no significant change or any pattern in the change in values at locations 2 and 4 in the X direction during these analyses.

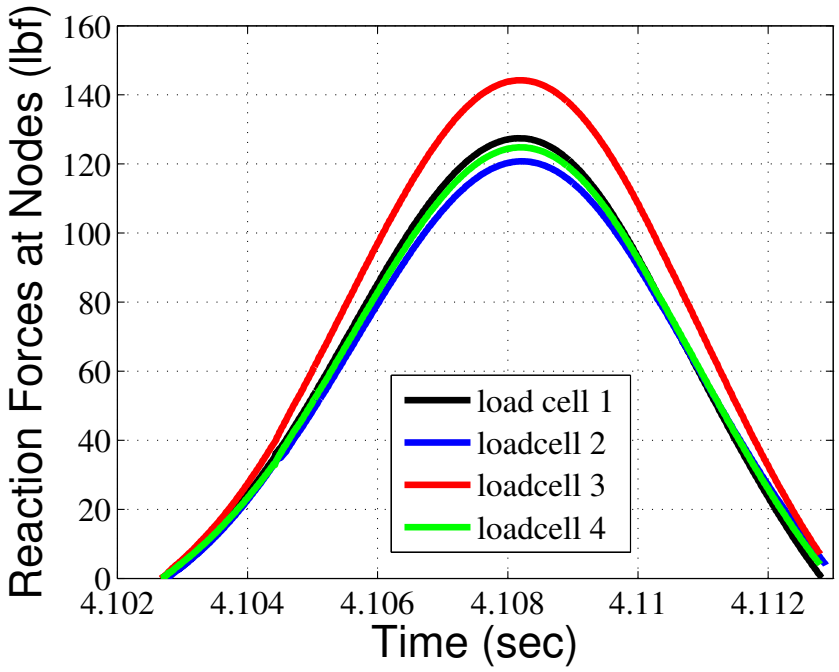

(a) Analysis with 1 mm Offset in X Direction

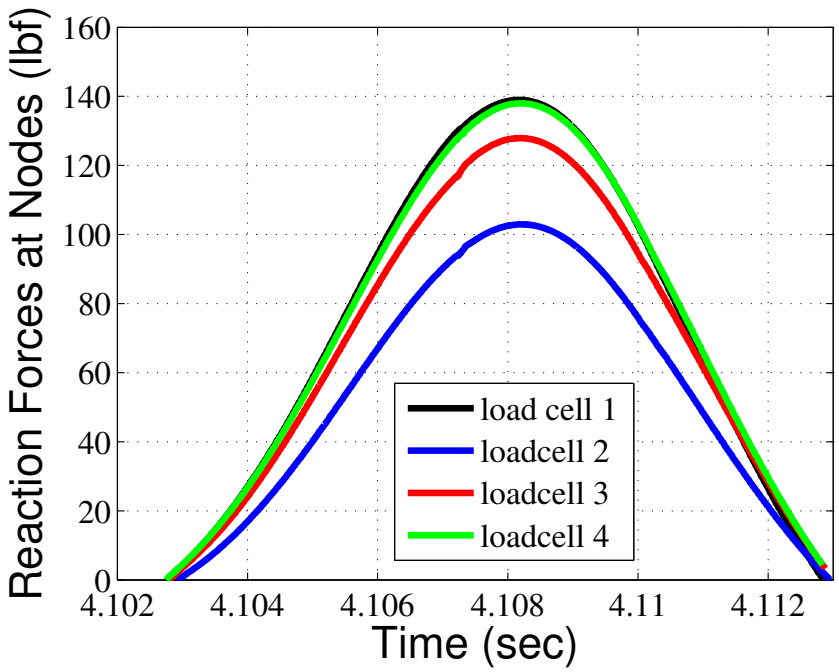

(b) Analysis with 5 mm Offset in X Direction

Figure 3.15.: Analysis with Offsets in X direction

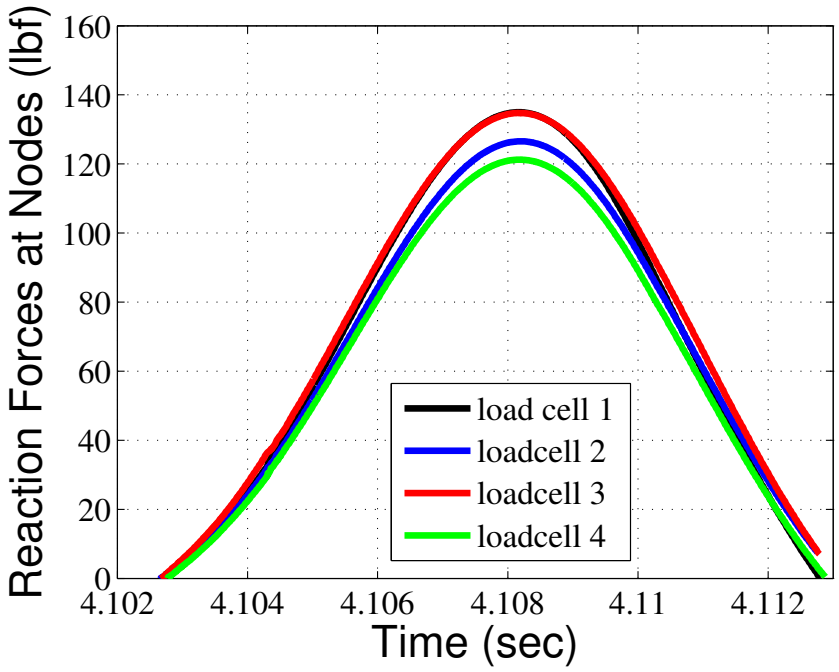

(a) Analysis with 1 mm Offset in Y Direction

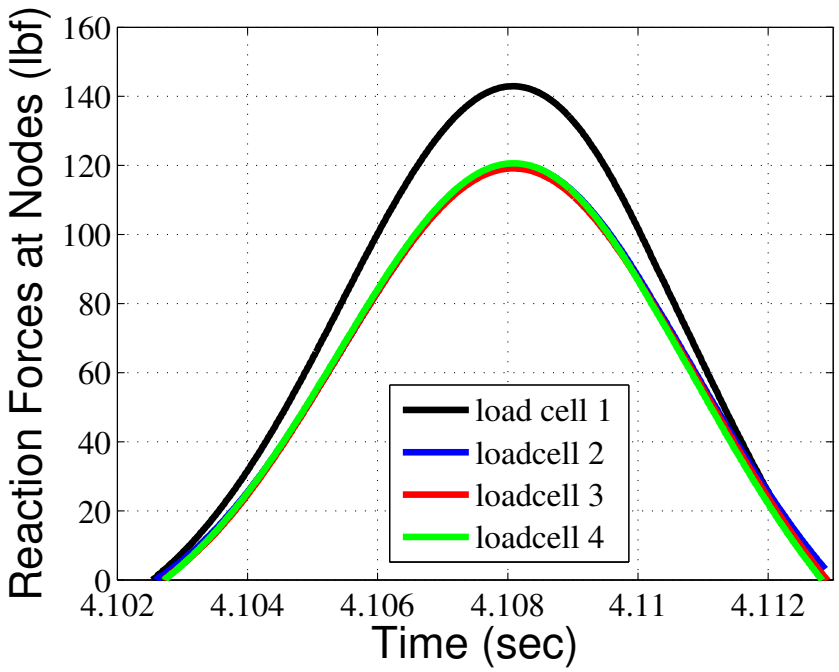

(b) Analysis with 5 mm Offset in Y Direction

Figure 3.16.: Analysis with Offsets in Y direction

Table 3.3.: Maximum Force Values at Every Load Cell Locations

Offset	Location 1(lbf)	Location 2(lbf)	Location 3(lbf)	Location 4(lbf)	Mean (lbf)	Std Dev(lbf)
Center of Mass	123.8	125.73	139.6	118.3	126.9	9.06
1 mm X offset	127.44	120.8	144.23	124.84	129.3	10.3
1 mm Y offset	135	126.56	134.78	121.26	129.4	6.7
5 mm X offset	139	103	127.9	138	126.9	16.75
5 mm Y offset	142.9	120.27	119.16	120.6	125.7	11.47

Table 3.3 shows the data for maximum force values for different offsets at different locations. Figure 3.17 shows the maximum force values at every load cell location for all the offsets. The values printed in red in the graph are used to indicate the major changes in the curves for that particular simulations. So the plots with X offset impacts show values at locations 2 and 4 marked in red, while plots with Y offsets show values at locations 1 and 3 marked in red to give more emphasis on these results. In order to simplify the description of these results, the standard deviation was plotted.

The huge variation of results by moving the impact point can be studied from this analysis. The maximum force value changes from 123.9 lbf in the reference simulation to 142.9 lbf for a 5 mm Y direction offset at location 1. Similarly the maximum force value changes from 118.3 lbf in the reference simulation to about 138 lbf for a 5 mm X direction offset. These differences of 19 lbf and 19.7 lbf respectively show the huge variation in the results with small offsets.

Figure 3.18 gives an idea of the standard deviation of the values for different offsets. The center of mass experiment showed a standard deviation of 9.06 due to the difference in force values owing to the lack of symmetry. Looking at the standard

deviation values for 5 mm offsets, showed the variation of values just by moving the impact point by small offsets.

The difference in the Standard Deviations showed the effect of small offsets on the entire simulation. Further, there were inconsistent changes in values that make generalization of the pattern difficult. These inconsistencies occurred due to lack of symmetry, errors in loading, difference in torque values while tightening bolts on the frames as well as slipping due to impact force overpowering the friction. Appendix D shows sensitivity analysis with frames constrained to move only in Z direction.

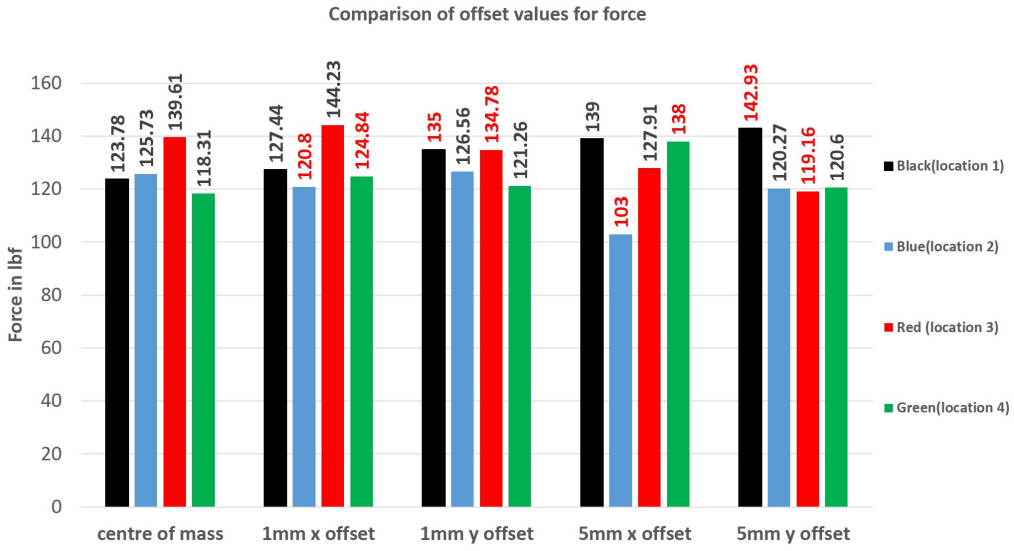

Figure 3.17.: Maximum Values of Force at Every Load Cell Location

A study of Fast Fourier Transforms was done in order to verify the difference in behavior at different load cells with offsets. For this study the Fast Fourier Transforms were plotted for the center of mass impact and 5 mm offset impacts in X and Y direction. The FFTs for the center of mass and 5 mm offsets from the sensitivity analysis are plotted in figure 3.19.

The FFT's were more or less similar for lower frequencies below 200 Hz. This was an expected phenomenon as the FFTs remain constant for the same matrial while

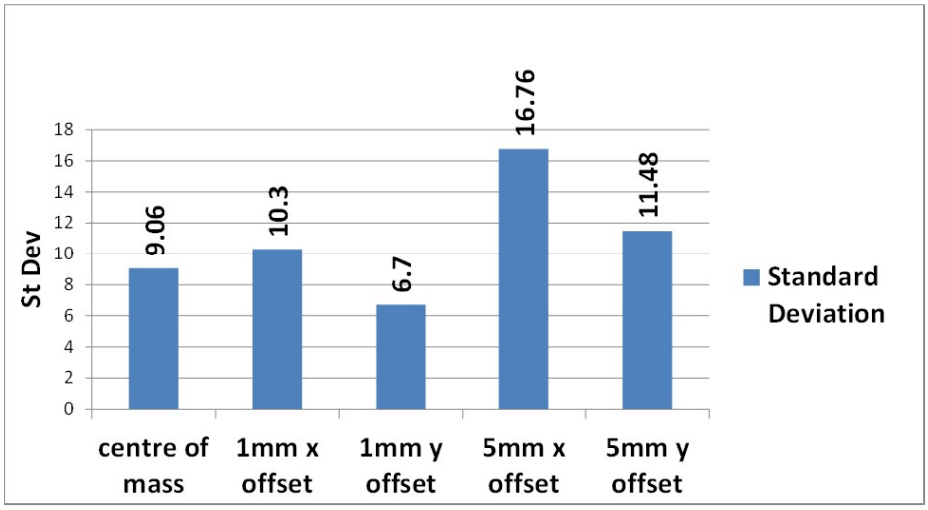

Figure 3.18.: Standard Deviation for Offsets

lower frequencies show the material influence. However, these FFT's show quite a variation for higher frequencies.

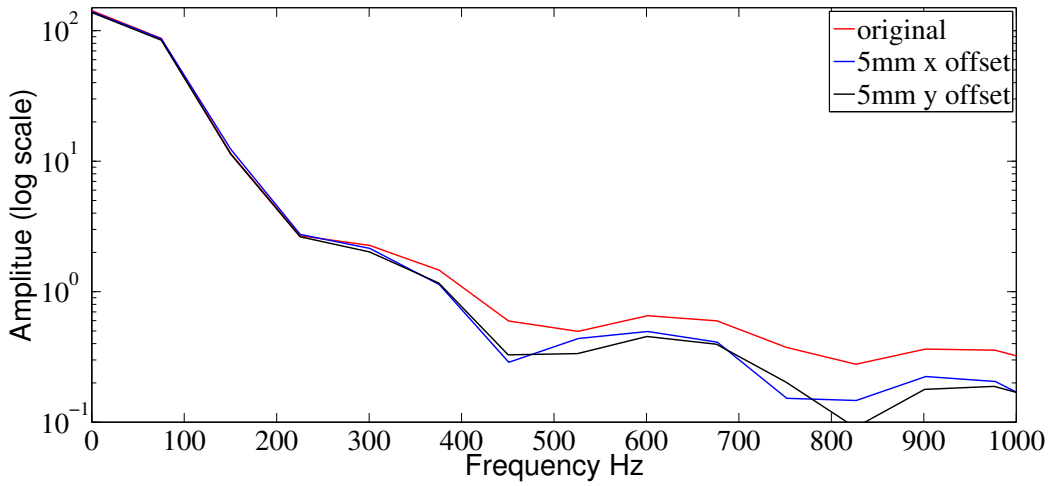

Figure 3.19.: Comparing Fast Fourier Transforms

These FFTs were considered to be an initial guess in making a distinction between a safe and unsafe vest. Even though more study was needed to understand the dynamics of these FFTs and analyse the behavior of these FFTs on impact, this analysis depicted the fact that these FFTs do not vary much based on the impact

locations. However, these FFTs showed quite a bit of difference in behavior for a study of different material which stated that the FFTs could be used in differentiating between different vests or between old and new vests. The FFTs for sensitivity analysis with constrained frames is shown in Appendix E

3.2.4 Influence of the Weight of the Frames

From a careful observation during the transition from Model 2 frame set-up to the Model 3, it was seen that the maximum force value ranges hiked from the older frame. This suggested the fact that the weight of the frame had some influence on the entire experiment.

In an attempt to study the effect of weight on the entire analysis, an analysis was planned to compare an experimental set-up with frames 44 lbs of mass with a set-up where the frames were non-existent. To achieve this, the frame with its original mass analysis was already available. In order to make the frames non existent while keeping the dynamics of the analysis same, a density of 10^{-20} magnitude was assigned to the frames which were initially given the density of steel i.e. $7.85\,\mathrm{g/cm^3}$. This gave a negligible mass to the frames, which is a requisite for ABAQUS to assign a non-zero density to every part.

Due to the variation in the load cell values, the mean values were considered for the analysis. Figure 3.20 shows the difference in simulation due to a difference in the weight of the frame. From the graph, the red curve shows the simulation with actual frame weight and the blue curve resembles the simulation with no frame weight. The fact that both curves got back to zero load at the same point of time, confirms the correctness of the analyses. The secondary peaks on the red curve were due to vibrations on the frames due to impact. Lack of these secondary peaks on the blue curve were due to no weight on the frames. This showed the huge influence of weight on the frames.

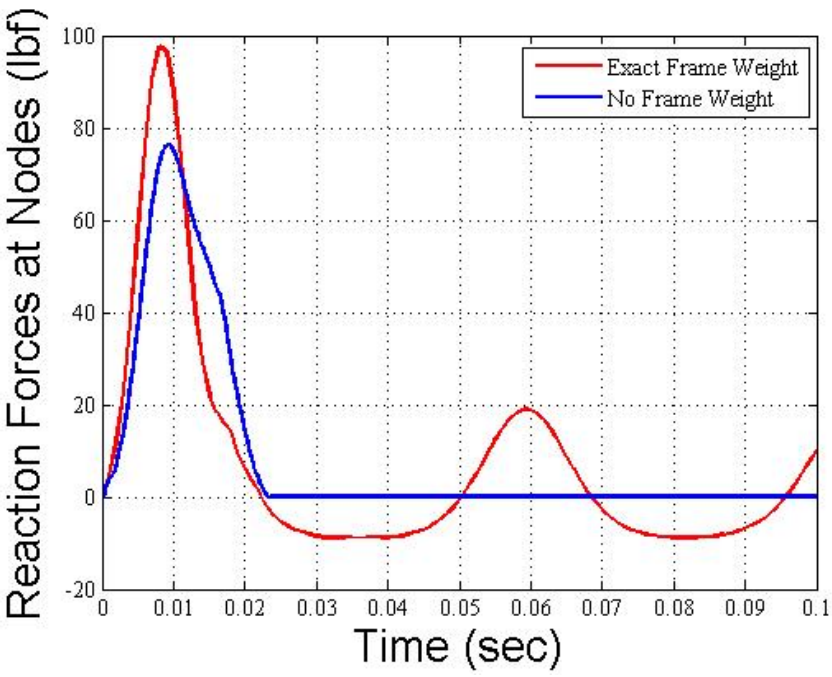

Figure 3.20.: Study of Influence of Weight on the Analysis

These results helped us validate the effectiveness of the set-up to replicate the actual experiment.

4. Conclusions

4.1 Evaluation of the Arrangement after Validation

The primary objective of this project was to help build an experimental set-up to validate the process of the drop tower/hammer impact. In this process, the Finite Element Model was intended to provide an accurate replica of the experimental set-up. In an attempt to accomplish this task, the evaluation of the validation process was provided in the following section.

A set of analyses were carried out during the course of this project to validate the experimental set-up using Finite Element Analysis. These experiments did not only provide the validation of the physics of the experiment, but also provided essential insights for the changes needed to be made in the on going set up to make it more robust, trustworthy and accurate. The following issues were encountered with Model 3.

The first main issue with the set up was the fact that the presence of the frames influenced the simulation results on a large scale. This was mainly because there was no boundary condition on the frames as they were freely resting on the load cells. The frames moved and vibrated after every impact shaking the entire set-up leading to disturbance in the force over time data making it very difficult to capture a pattern in the impact analysis.

A set of simulations were run with constrained boundary conditions such that the frames moved only in Z-direction. This was an attempt to generalize the behavior of impact. This made the movement of the frames less random. These results are shown in appendix B.

The freely resting frames being 44 lbs in weight had a huge weight influence on the set-up. On impact, the load cell managed to record a reaction force which was a

combination of impact and self weight as the frames were just rested on the load cells. This influence of weight of the frames led to inaccuracy in replicating the experiment. The next issue with the current set up was the lack of symmetry. Even with constrained frames, different load cell locations would capture different reaction forces due lack of symmetry about the X-axis. This made it necessary to consider the mean values for comparison which did not bring out the actual physics of the behavior of materials. Another issue recorded with this set-up was the location of the load cells. Owing to the lack of symmetry, positioning the load cells along X and Y directions led to huge differences in force values at these load cells.

Further, a minor difference between the experimental set-up and the Finite Element Analysis stated that there was a lot of noise in recoding the experimental values. It was found that this noise was due to the movement of the long impactor rod while free falling due to gravity as the rod moved laterally during its stride downwards.

Finally, the center of mass of the entire set-up kept changing due to changes in the number of bolts used to tighten the frames. So a better clamping process was needed for the frames in order to hold the sample in between them.

4.2 Proposed Arrangement

Studying the shortcomings of the the ongoing arrangement used, the new proposed set-up needed the following changes:

- This new set-up needed frames that would be symmetric about both X and Y axes.
- A mechanism that would hold both the frames in their position to prevent their movement after the first impact.
- A different mechanism to hold the frames tightly in their spot with the vest well clamped in between.

- The location of load cells diagonally along the frames, equidistant from the center.
- A well guided impactor based on applied force or velocity.

5. Current and Future Work

5.1 Improved Experimental Arrangement - Current Work

After a careful consideration to the changes suggested in the Conclusions, the new experimental set-up was built as follows:

- The top and bottom frames manufactured for the new set-up were square shaped with a circular cut test section in the center, 24 in by 24 in in dimensions with a thickness of 0.5 in.
- The bottom frame was fixed and was not allowed to move while the top frame was given a downward force of 105 lbf using actuators controlled by pressure at 4 locations equidistant from the center to hold it from moving after impact.
- A square Aluminium plate 12 in by 12 in in dimensions and 0.0625 in thick, was used for analysis in place of a steel plate which was placed at the center of the frame.
- The impactor was given a pressure of 50 psi using a pressure controlled valve and dropped from a height of 2 in and retracted back after impact to consider just the first impact.
- The load cells were positioned diagonally from the center of the circlular cut at 2.1 in from the center which records the reaction forces.
- An input force was recorded using the actuator on the impactor.
- The actuators were mounted on a robust fixture showed in figure 5.1.

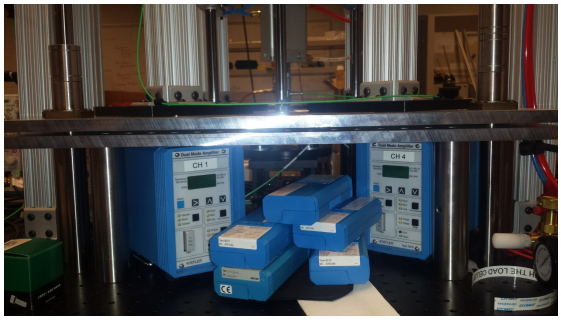

(a) Side View of the Plates and Actuator Set-up

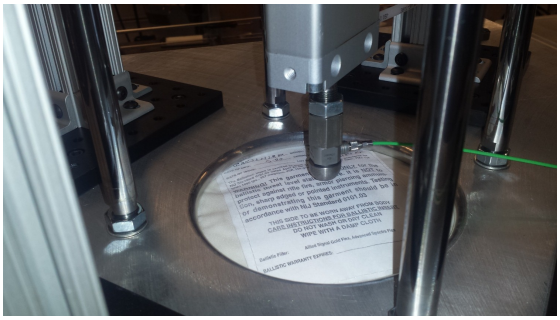

(b) Impactor Controlled by Actuator

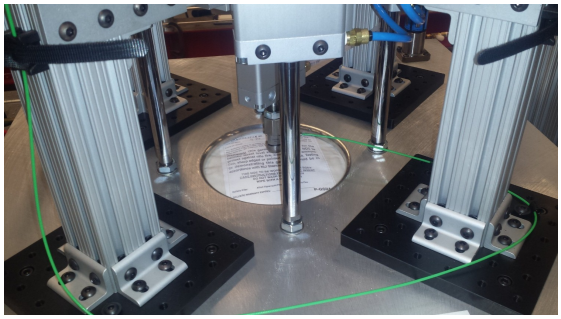

(c) Actuators used

(d) Pressure Controlling Valves

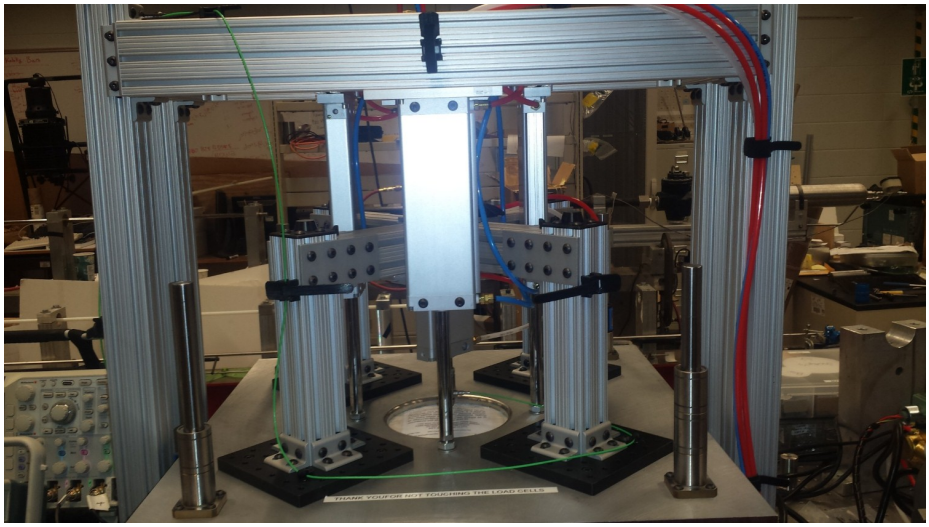

(e) New Experimental Set-up

Figure 5.1.: Improved Experimental Arrangement

Figures 5.2 shows this result recording force over time for the experiment using the new set-up. The results of the analysis were plotted showing the total output force on all load cells (black curve) and the input force as shown by the actuator on the impactor (red curve). The black curve showing the maximum force value in the entire time frame goes to about 88 lbf. This is almost 25% of the total output force as in case of the previous arrangements which stresses the removal of influence of the frame weight. The input force is lesser than the output force even though both the curves are aligned. This is due to the reaction given by the steel plate adds to the reaction force on the load cells.

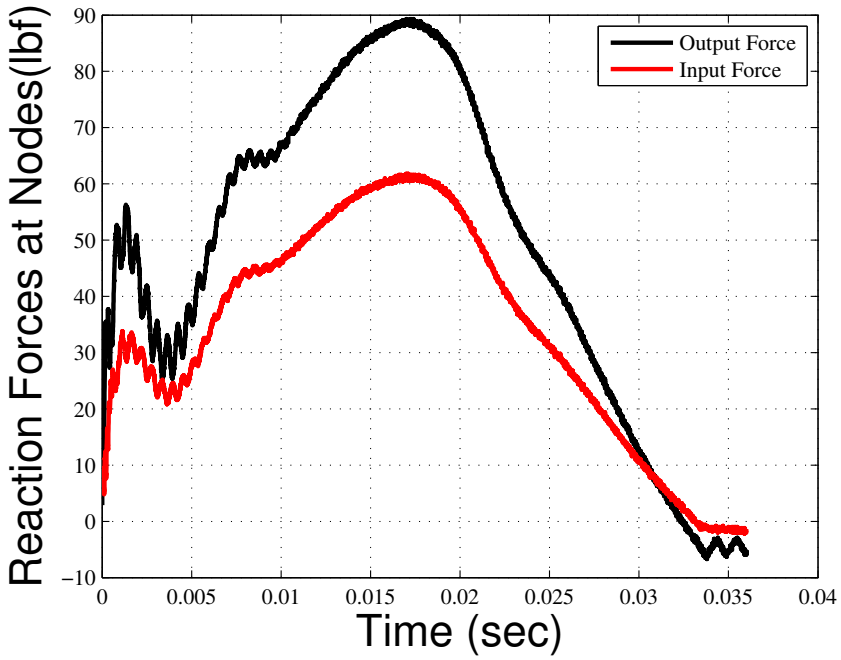

Figure 5.2.: Input and Output Forces Recorded on the New Set-up

5.2 Finite Element Model for the New Set-up

The Finite Element Model for the new experimental set-up was built similarly as in case of the previous arrangement. It consisted of the same 5 parts including the top and bottom frames, an aluminium plate, the impactor and four load cells.

Top and Bottom Frames: The top and bottom frames were made of mild steel with a young's modulus of 210 Gpa and a Poisson's ratio of 0.3. These frames had a circular cut of radius 3 in in the center which formed the test section. These square plates were assigned a swept mesh with Explicit, Linear and Hexahedral elements of size 30 mm. This element size kept the geometry of the frames impact. Further, the frames were made rigid as they did not influence the simulation apart from holding the plate in it's place. These frames are seen in figure 5.3

Aluminium Plate: As preferred for experimental analysis, an aluminium square plate was used in this analysis with a young's modulus of 70 Gpa, Poisson's ratio of 0.33 and a density of 2700 kg/m^3 This plate was assigned a Swept mesh with Explicit, Linear Elements with a mesh size of 10 mm overall and 2 mm in the test section. Figure 5.4 shows the steel plate modelled in simulation.

Load Cells: The load cells were made of steel with the same properties as the frames. These load cells were also assigned an Explicit, Linear Hexahedral elements of size 1 mm. This element size gave accurate simulations with optimum computational time as any small element size gave same results with more computational time. 4 such load cells were used in the set-up placing the frame and plate arrangement resting on the load cells. The load cells modelled in ABAQUS are shown in figure 5.5

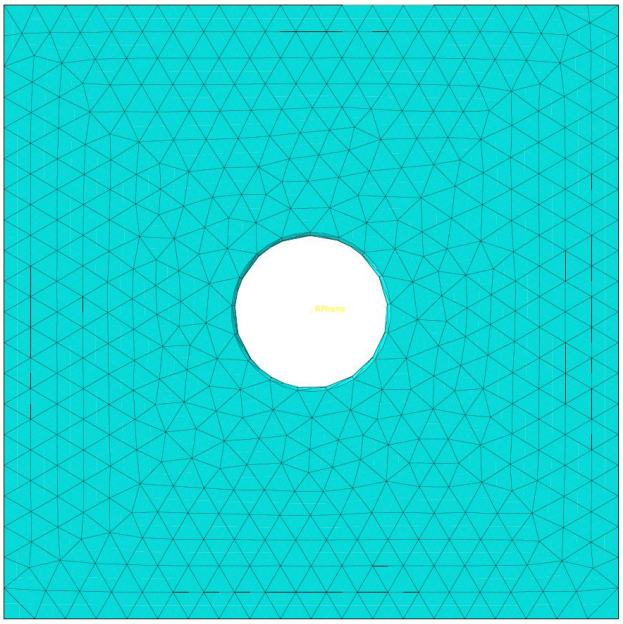

(a) Frame Geometry in Top View

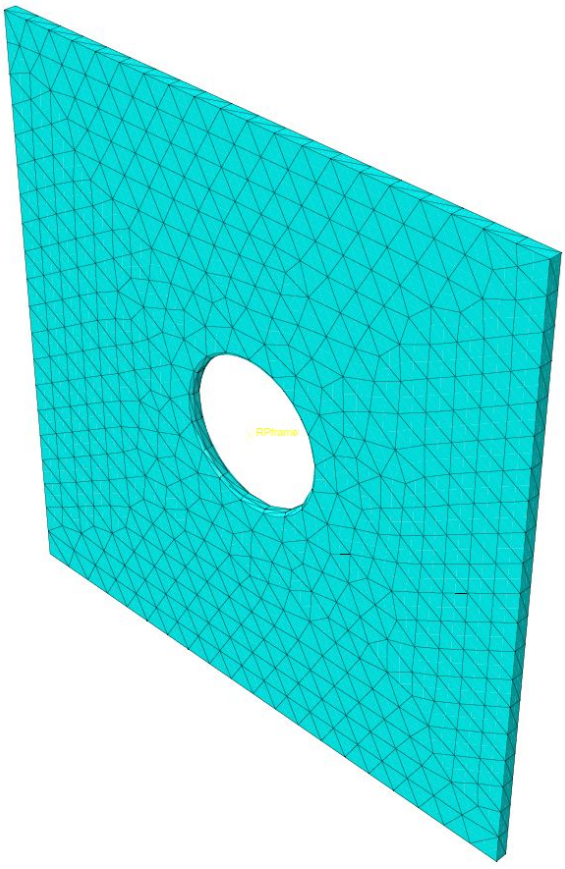

(b) Frame Geometry in Isometric View

Figure 5.3.: Finite Element Model of the Frame

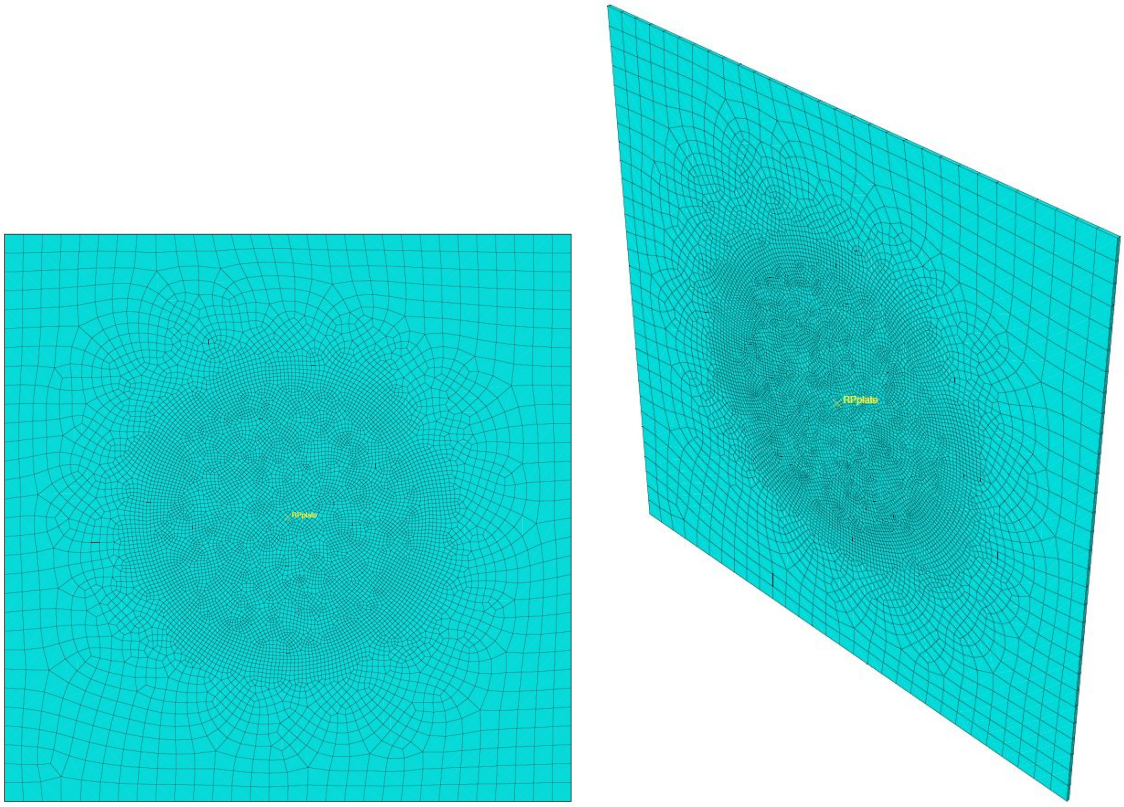

(a) Plate Geometry in Top View (b) Plate Geometry in Isometric View

Figure 5.4.: Finite Element Model of the Aluminium Plate

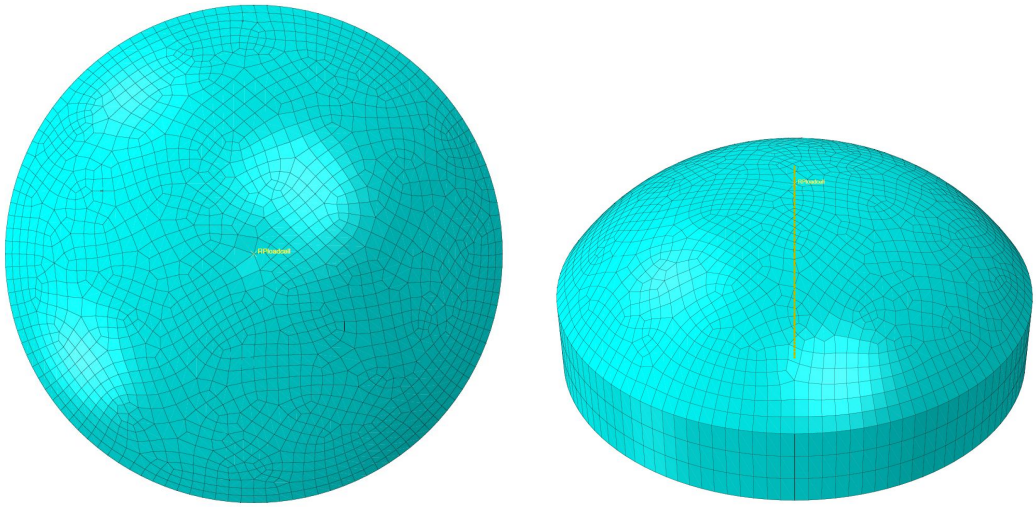

(a) Load Cell Geometry in Top View (b) Load Cell Geometry in Isometric View

Figure 5.5.: Finite Element Model of the Load Cells

Impactor: The impactor used in the Simulation was same as that in case of the previous model. It was assigned to be an analytical rigid body which again saved the computational time due to lack of need for meshing. The impactor figure is shown in figure 5.6

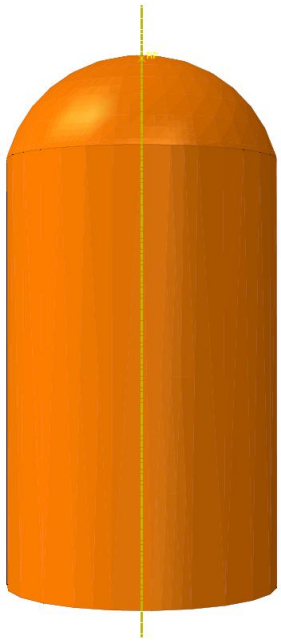

(a) Impactor Geometry in Top View

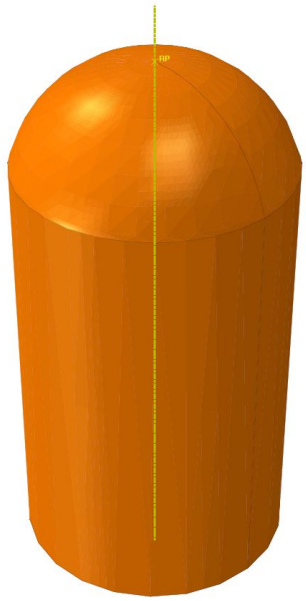

(b) Impactor Geometry in Isometric View

Figure 5.6.: Finite Element Model of the Impactor

These parts were then assembled and given the following process parameters to replicate the physics of the actual experiment in the Finite Element Analysis.

- Both the frames with the aluminium plate were imported in the assembly and aligned such that the center of geometries (also the center of mass) of the frames and plates were along the same X and Y coordinates with the plate sandwiched in between the frames.
- The four load cells were then imported and aligned such that they were placed diagonally from the center of the plate at 2.1 in distance. These load cells were brought just in contact with the plate on its bottom .
- The impactor was brought just in contact with the plate on the top surface alinged along the Z direction.
- This simulation did not need the self weight vibration step as the frames were constrained which saved most of the computational time.
- A Normal Behavior with Hard Contact was the interaction used (default interaction) on all surfaces in contact as the number of surfaces involved were not too many.
- The top and bottom frames were made rigid and they were tied to the plate with their respective surfaces in contact to make sure the plate did not move after impact.
- A force of -23. N was assigned to the impactor as the load in place of just gravitational force.
- The two frames and load cells were assigned the encastre condition that prevents them from moving while the impactor is allowed to only move in the Z-direction.

This is how the arrangement was set in ABAQUS.

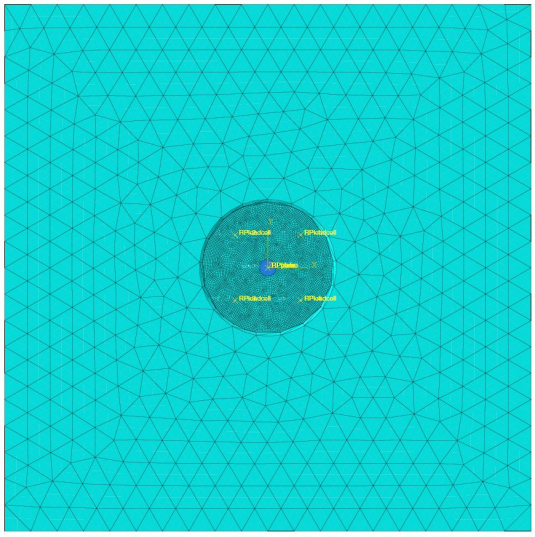

(a) Finite Element Mode Assembly in Top View

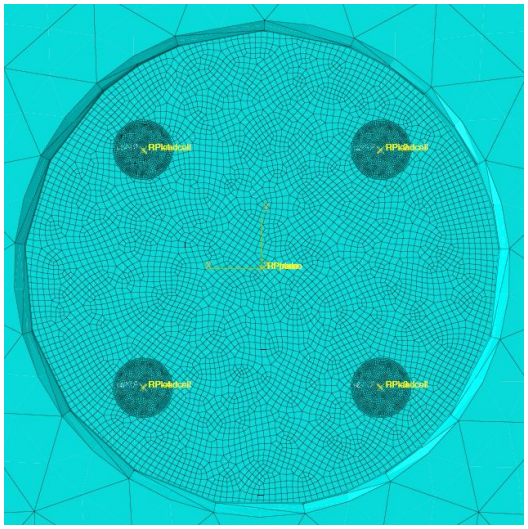

(b) Test Section in Bottom View

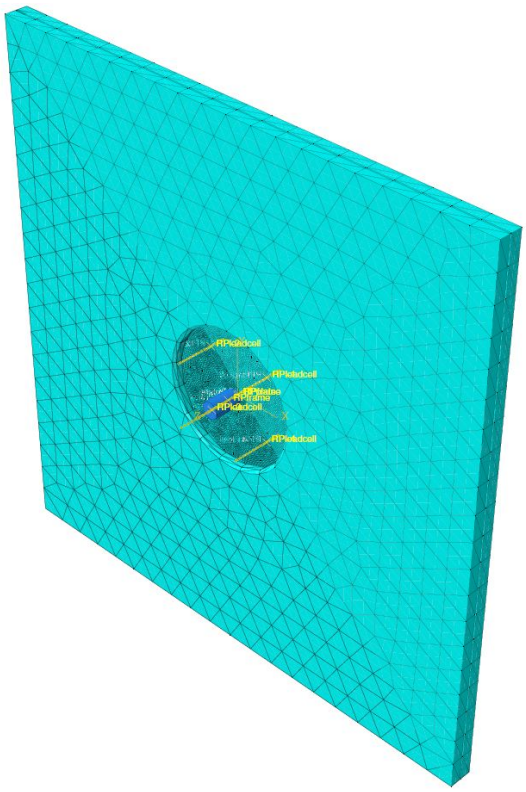

(c) Finite Element Mode Assembly in Isometric View

Figure 5.7.: Finite Element Model of the New Set-up

Attempts are being made to run the simulation with the process parameters exactly same as the experimental set-up.

5.3 Future Work

The main intention of this project is to build a portable Non-Destructive testing apparatus that could be carried to any location where a vest could be tested in minutes giving out a Go-No-Go on the safety of the jackets. In order to achieve a completion of this project, it is necessary to validate the current procedure used and carry on with testing the vest fabric using the same finite element model and understand the dynamics of the vest, which would be quite different from that of an aluminium/steel plate.

The main task as the next step towards this project was to build a homogeneous fabric model in ABAQUS that could be used directly in every simulation for every material, that is used to make the vest, just by entering their ply properties. In order to build a homogeneous model, it was necessary to study the properties of the fabric used. Due to the fact the single ply properties of different materials were not readily available, it was necessary to obtain these properties through experimental analyses or Finite Element Analysis. Since it was time consuming to carry out experimental analysis on all new fabrics, it was simpler to build a finite element model to carry out simulations determining the fabric properties.

An initial guess in the direction to build a fabric model was to obtain fiber or yarn properties and level up to a fabric. In an attempt to do so, it was realized that levelling up from a fiber model was not feasible due to the number of fibers in a single ply. So in order to level up from a yarn level, it was planned to use a software package called TexGen to build this yarn model. TexGen takes care of the yarn width, yarn spacing as well as yarn interactions.

This TexGen file was then planned to be imported to ABAQUS for further study. The plan was to carry out simple tests including Tensile, Compression, Shear and

other such tests in order to find out the properties required to set up the fabric model. Figure 5.8 shows the preliminary yarn model imported to ABAQUS. This TexGen model had yarns with 0.2 mm width and 0.8 mm length. The material interactions were taken care off by the TexGen software. Fibres were constrained to not move in the X direction along one axis and pulled with a pressure of 1Mpa on the other side. Figure 5.9 shows the behavior due to this tensile test. This was just the preliminary steps to try and understand the boundary conditions. Further study is needed to understand these concepts.

The next few steps towards the completion of the project include:

- Carry out required analysis on the yarn models to obtain properties of materials/fabrics.
- Try to build a fabric model that takes aging into account.
- Build the apparatus based on correlation of results from Experiment and Finite Element Analysis.

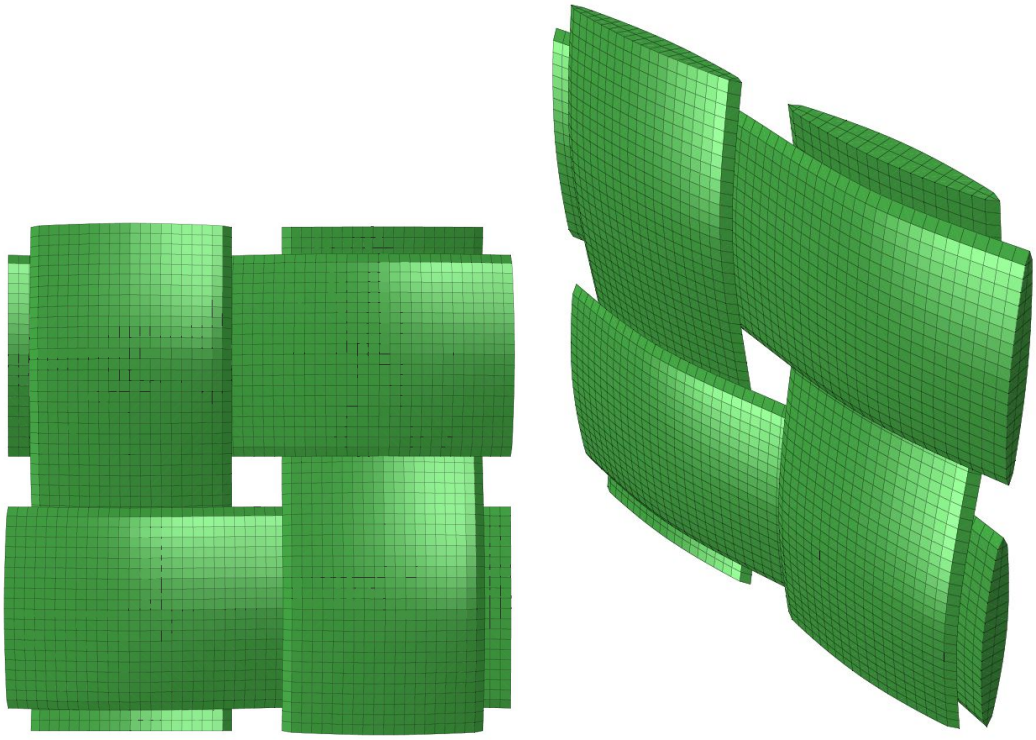

(a) TexGen Model in Top View (b) TexGen Model in Isometric View

Figure 5.8.: Glimpse of TexGen Model in ABAQUS

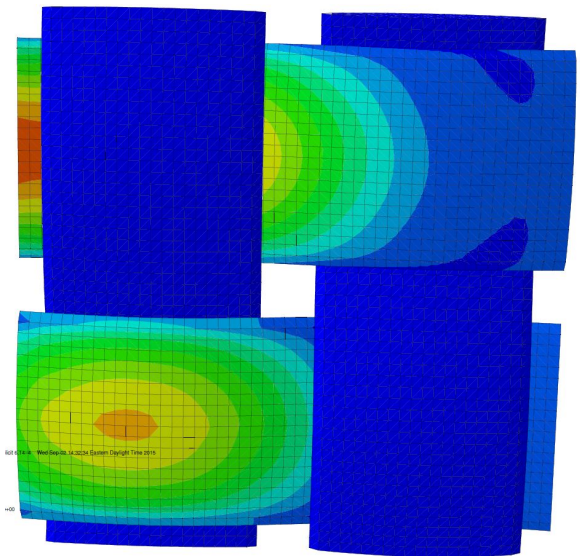

Figure 5.9.: Simple Tensile Load on One End and Constrained on Other

REFERENCES

REFERENCES

[1] M. Hudspeth, B. Claus, N. Parab, and W. Chen. *Proposed Non-Destructive Evaluation Test Method of Soft Body Armor Types I-III*. National Institute of Justice, Proposal Number: 2014-MU-CX-K004 edition.

[2] National institute of justice guide: Body armor - 247281. `https://www.ncjrs.gov/pdffiles1/nij/247281.pdf`.

[3] Kobi Peleg, Avraham Rivkind, Limor Aharonson Daniel, and the Israeli-Trauma Group. Does Body Armor Protect from Firearm Injuries? *Journal of the American College of Surgeons. Volume 202*, 2006.

[4] U.S. Congress Office of Technology Assessment. *Police Body Armor Standards and Testing Vol. I.* U.S. Government Printing Office, August 1992.

[5] Fbi uniform crime reports 2011- law enforcement officers killed and assaulted (leoka) table 70. `http://www.fbi.gov/about-us/cjis/ucr/leoka/2011`, 2011.

[6] Fbi uniform crime reports 2011- law enforcement officers killed and assaulted (leoka) tables 1 and 38. `http://www.fbi.gov/about-us/cjis/ucr/leoka/2011`, 2011.

[7] LaTourrette T. The Life-Saving Effectiveness of Body Armor for Police Officers. *Journal of Occupational and Environmental Hygiene. pg 557-562*, 2010.

[8] Sgt. Stanley Muszynski. Body Armor. Technical report, Eastern Michigan University - School of Staff and Command, August 19 2004.

[9] Deidre Di Liddo and Emma George Hewett. BODY ARMOR. `http://www.scientiareview.org/pdfs/260/`.

[10] History of bulletproof vests. `http://www.bulletsafe.com/the-history-of-bulletproof-vests.html`.

[11] Body armor classifications. `http://www.globalsecurity.org/military/systems/ground/body-armor1.htm`.

[12] US Department of Justice. *Ballistic Resistance of Personal Body Armor 0101.06*, 6th Edition edition, 2008.

[13] M. Heideman, D.H. Johnson, and C.S. Burrus. Gauss and the history of the fast fourier transform. *ASSP Magazine, IEEE*, 1(4):14–21, October 1984.

[14] Gilbert Strang. *Wavelets*. Sigma Xi. The Scientific Research Society, 1994.

[15] J. Dongarra and F. Sullivan. Guest editors introduction to the top 10 algorithms. *Computing in Science Engineering*, 2(1):22–23, Jan 2000.

[16] Charles Van Loan. *Computational Frameworks for the Fast Fourier Transform.* Society for Industrial and Applied Mathematics, 1992.

[17] X. Zeng, V. Shim, and V. Tan. Finite-element modeling of the ballistic impact of fabric armor. *International Journal of Impact Engineering 32 pg. 631*, 2005.

[18] H. Shin, D. Erlich, and D. Shockey. Ballistic Impact of Dry Woven Fabric Composites. *Journal of Materials Science 38 pg. 3603*, 2003.

[19] Ming Cheng and Weinong Chen andTusit Weerasooriya. Experimental investigation of the transverse mechanical properties of a single KevlarKM2 fiber. *International Journal of Solids and Structures.Vol 41. Issues 2223.Pg 6215-6232*, November 2004.

APPENDICES

Appendix A: Matlab script for the example of Fast Fourier Transforms of a Sine Wave

The matlab script below shows how a simple sine wave is converted to its Power Spectrum using the Fast Fourier Transforms.

```
Fs = 150;              % Sampling frequency
t = 0:1/Fs:1;          % Time vector of 1 second
f = 5;                 % Create a sine wave of f Hz.
x = sin(2*pi*t*f);
nfft = 1024;           % Length of FFT
X = fft(x,nfft);       % Take fft, padding with zeros so that length(X)
                       % is equal to nfft
X = X(1:nfft/2);       % FFT is symmetric, throw away second half
mx = abs(X);           % Take the magnitude of fft of x
f = (0:nfft/2-1)*Fs/nfft;    % Frequency vector
figure(1);             % Generate the plot, title and labels.
plot(t,x);
title('Sine Wave Signal');
xlabel('Time (s)');
ylabel('Amplitude');


figure(2);
plot(f,mx);
title('Power Spectrum of a Sine Wave');
xlabel('Frequency (Hz)');
ylabel('Power');
```

Appendix B: Force over Time for 0.5 m/s Velocity without Self Weight Vibrations

This figure shows the simulation for the First Attempt with no consideration of self weight vibration for a velocity of 0.5 m/s. This velocity was assigned by dropping the impactor from a height of 0.5 in. Figure B.1 shows this plot where the behavior is similar to the plot for impact with 1 m/s velocity with respect to the disturbances observed.

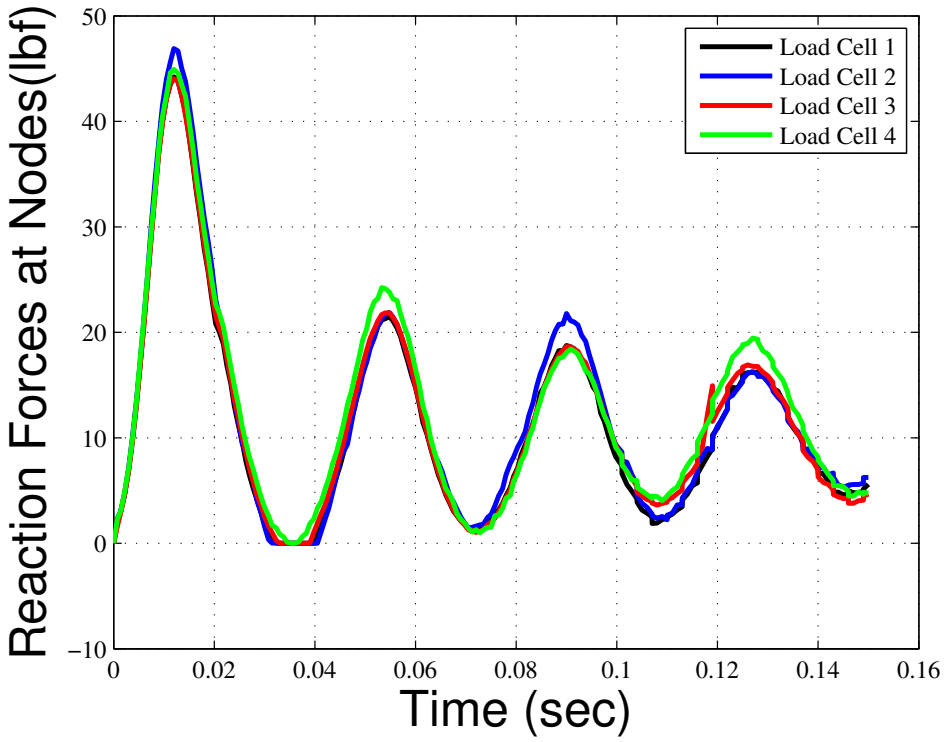

Figure B.1.: Force over Time for 0.5 m/s Velocity without Self Weight Vibrations

Appendix C: Comparison of Different Materials with Constrained Frames

The first attempt to compare different materials was carried out by assigning boundary conditions on the frames such that they move only in the Z direction. This follows a similar behavior to the analysis with frames allowed to move in all directions in terms of peaks of maximum force and the time taken to reach the peak.

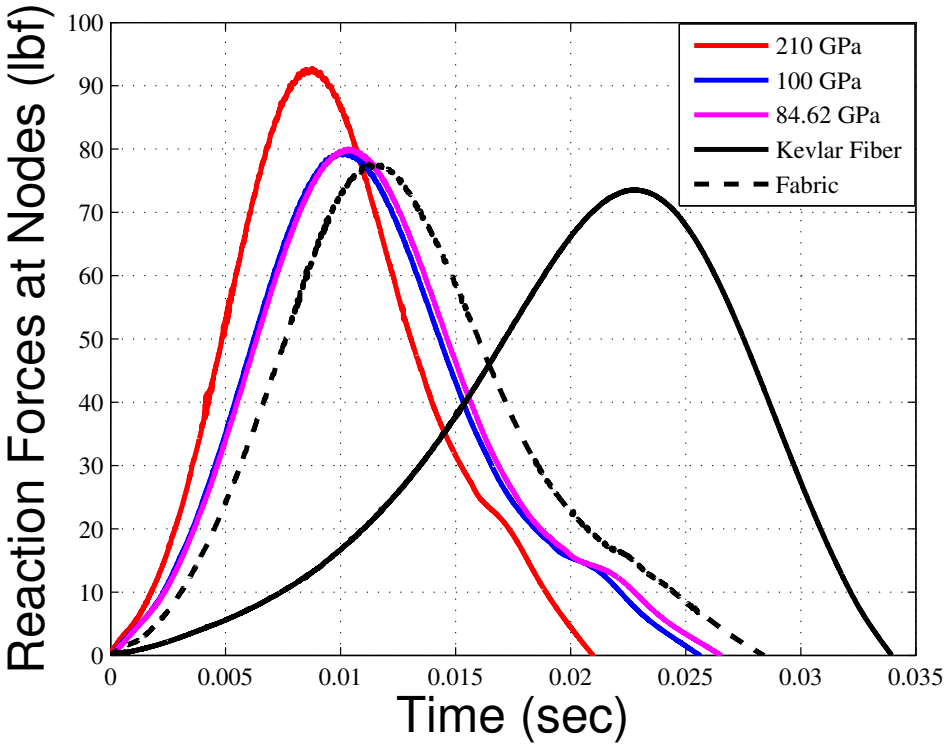

Figure C.1.: Comparison of Different Materials with Frames Constrained to Move in Z Direction

Appendix D: Sensitivity Analysis with Constrained Frames

This section shows sensitivity analysis with frames constrained to move only in Z direction

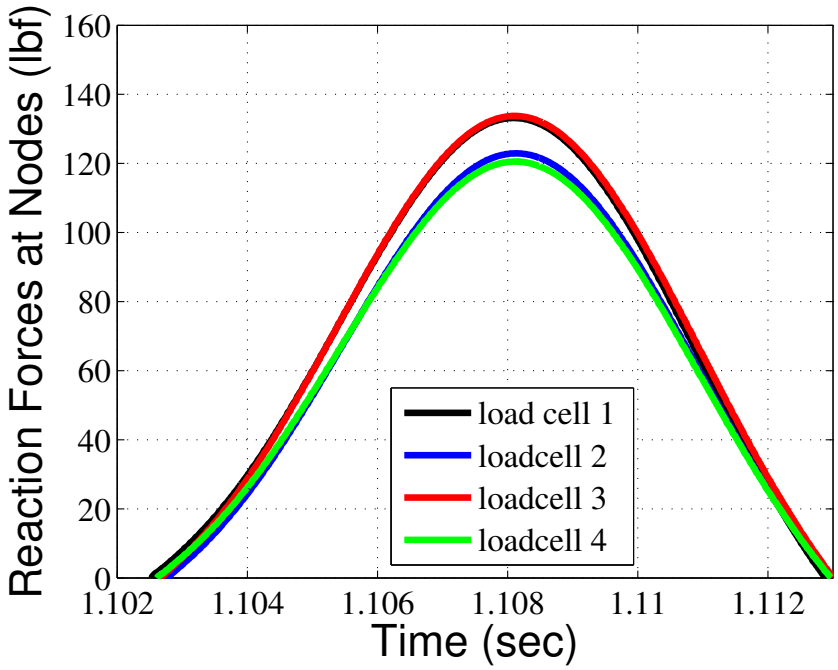

Figure D.1.: Benchmark for Comparison - Impact at Center of Mass

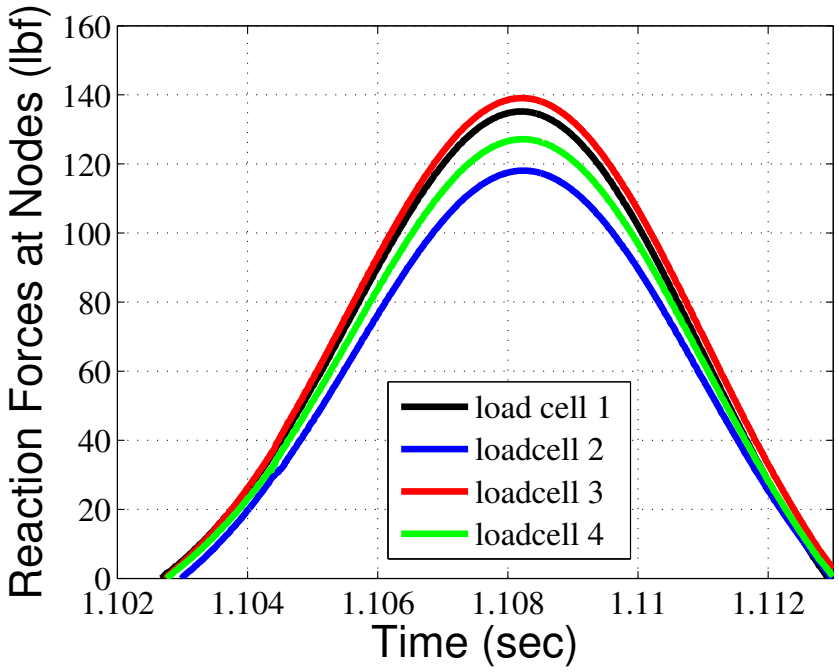

(a) Analysis with 1 mm Offset in X Direction

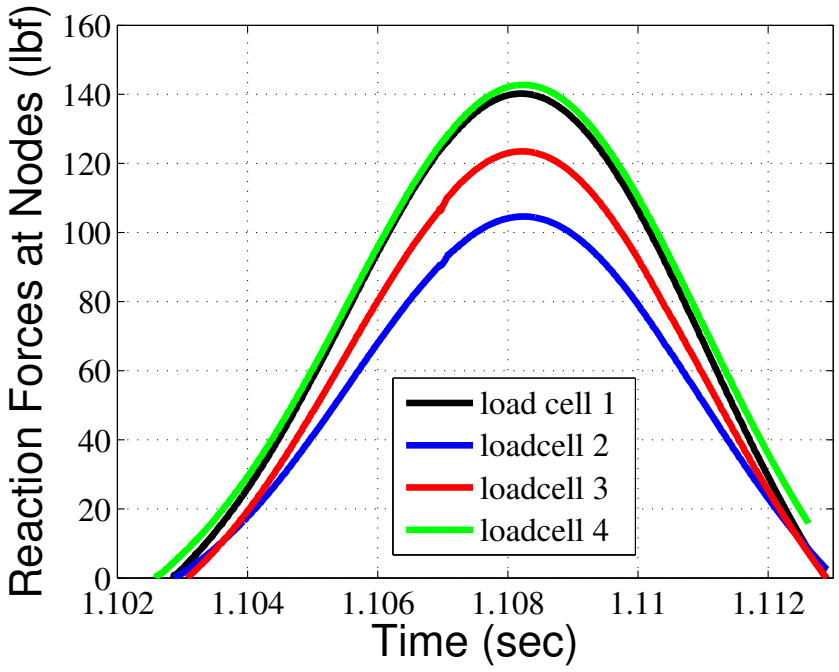

(b) Analysis with 5 mm Offset in X Direction

Figure D.2.: Analysis with Offsets in X direction

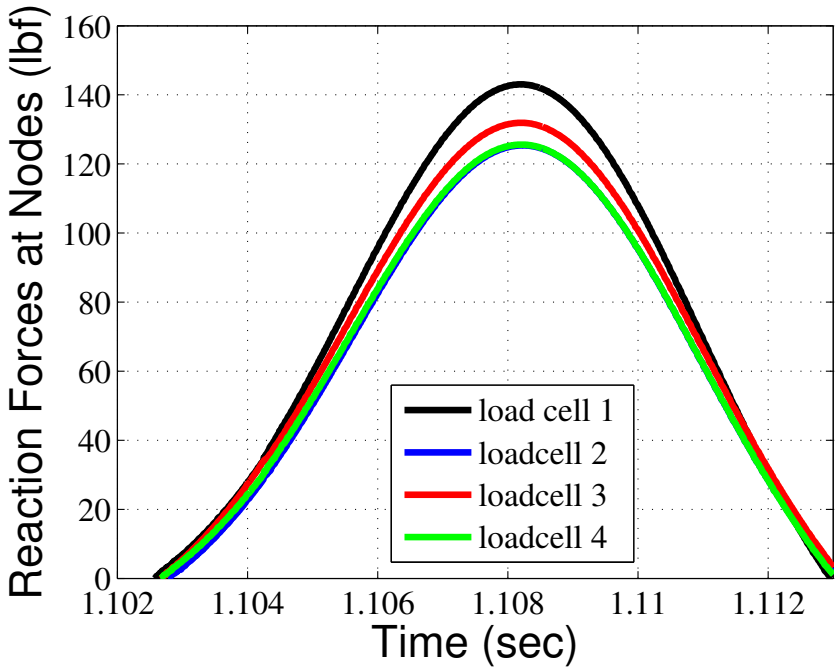

(a) Analysis with 1 mm Offset in Y Direction

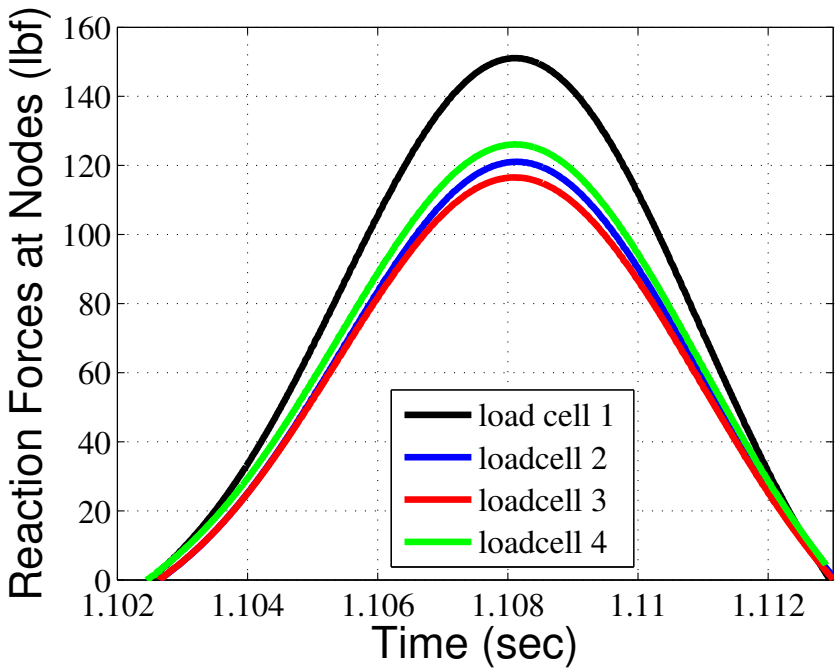

(b) Analysis with 5 mm Offset in Y Direction

Figure D.3.: Analysis with Offsets in Y direction

Figure 3.17 shows the maximum force values at every load cell location for all the offsets.

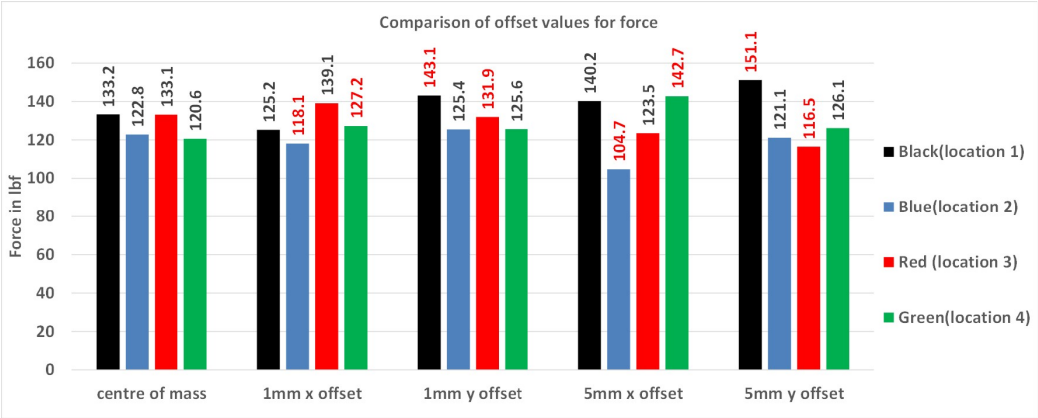

Figure D.4.: Maximum Values of Force at Every Load Cell Location

The values printed in red in the graph show the variation from the center of mass values when impact is offset in the corresponding direction of the locations. Figure D.5 gives an idea of the standard deviation of the values for different offsets.

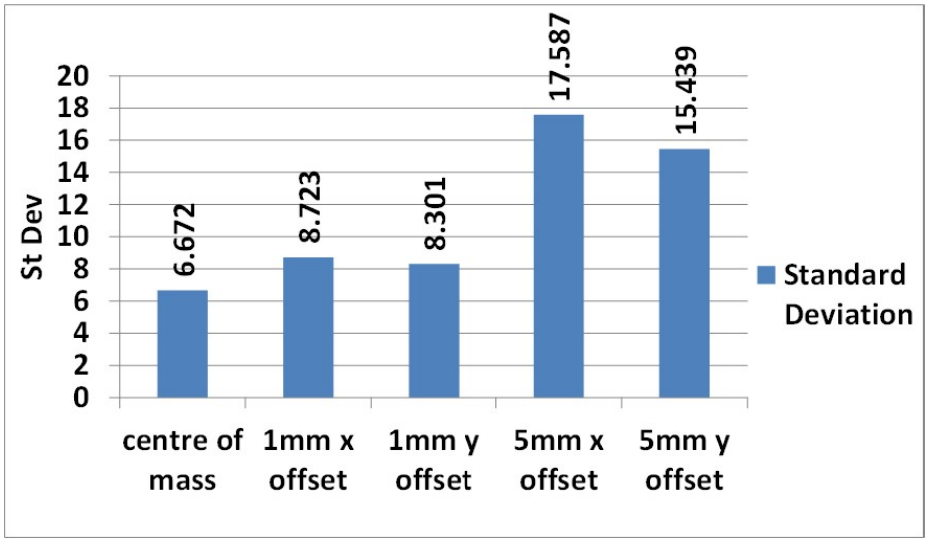

Figure D.5.: Standard Deviation for Offsets

Table D.1.: Maximum force values at Every Load Cell Locations

Offset	Location 1(lbf)	Location 2(lbf)	Location 3(lbf)	Location 4(lbf)	Mean (lbf)	Std Dev(lbf)
Center of Mass	133.2	122.8	133.1	120.6	127.4	6.67
1 mm X offset	125.2	118.1	139.1	127.2	127.4	8.72
1 mm Y offset	143.1	125.4	131.9	125.6	131.5	8.3
5 mm X offset	140.2	104.7	123.5	142.7	127.7	17.6
5 mm Y offset	151.1	121.1	116.5	126.1	128.7	15.44

Appendix E: Fast Fourier Transforms for Sensitivity Analysis with Constrained Frames

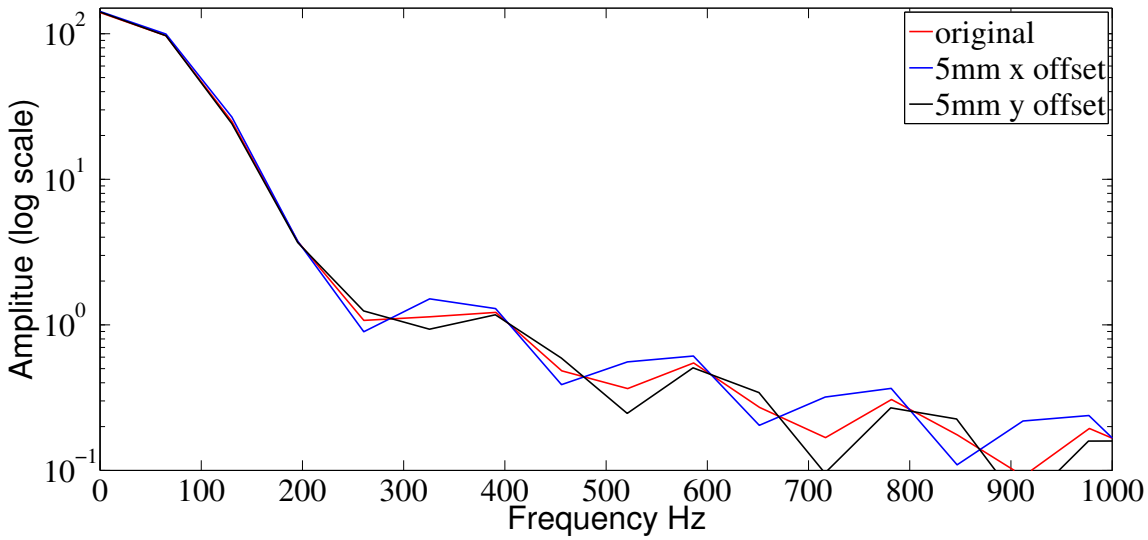

Figure E.1.: Fast Fourier Transforms Comparison for Offsets